Fábio Retorta, João Mello, Clara Gouveia, Bernardo Silva, José Villar, Matteo Troncia, José Pablo Chaves-Ávila, Local flexibility markets based on grid segmentation, Utilities Policy, Volume 96, 2025, 102029, ISSN 0957-1787, https://doi.org/10.1016/j.jup.2025.102029


```
@article{RETORTA2025102029,
title = {Local flexibility markets based on grid segmentation},
journal = {Utilities Policy},
volume = {96},
pages = {102029},
year = {2025},
issn = {0957-1787},
doi = {https://doi.org/10.1016/j.jup.2025.102029},
url = {https://www.sciencedirect.com/science/article/pii/S0957178725001444},
author = {Fábio Retorta and João Mello and Clara Gouveia and Bernardo Silva and José Villar and Matteo Troncia and José Pablo Chaves-Ávila},
keywords = {Active power flexibility, Distribution grid constraints, Grid segmentation, Linear optimization, Local flexibility markets},
```

Local Flexibility Market based on Grid Segmentation

Fábio Retorta[a,b*)], João Mello[a,b], Clara Gouveia[a,], Bernardo Silva[a,b], José Villar[a,], Matteo Troncia[c], José Pablo Chaves-Ávila[c]

[a)] Institute for Systems and Computer Engineering Technology and Science (INESCTEC), Dr. Roberto Frias, 4200-465, Porto, Portugal

[b)] Faculty of Engineering of the University of Porto, Dr. Roberto Frias, 4200-465, Porto, Portugal

[c)] Institute for Research in Technology (IIT), ICAI School of Engineering, Universidad Pontificia Comillas, C/del Rey Francisco 4, 28008 Madrid, Spain

[*)] Corresponding author: fabio.retorta@inesctec.pt

Abstract

Local flexibility markets are a promising solution to aid system operators in managing the network as it faces the growth of distributed resources and the resulting impacts on voltage control, among other factors. This paper presents and simulates a proposal for an intra-day local flexibility market based on grid segmentation. The design provides a market-based solution for distribution system operators (DSOs) to address near real-time grid issues. The grid segmentation computes the virtual buses that represent each zone and the sensitivity indices that approximate the impact of activating active power flexibility in the buses within the zone. This allows DSOs to manage and publish their flexibility needs per zone and enables aggregators to offer flexibility by optimizing their resource portfolios per zone. The simulation outcomes allow for the assessment of market performance according to the number of zones computed and show that addressing overloading and voltage control through zonal approaches can be cost-effective and counterbalancing small errors compared to node-based approaches.

Keywords

Active power flexibility; distribution grid constraints; grid segmentation; linear optimization; local flexibility markets

Nomenclature

Indexes:

$i,j,n,$	Node/Bus
L	Branch
Nc	Matrix line
Vb	Virtual bus
v,i	Voltage and current
Gel	Grid elemen
Q	Problematic element
z	Grid zone (zone number)
z_{vb}	Virtual bus of zone z
K	Flexibility service provider (FSP)
B	Base
C	Cluster number
q_b	Problematic bus element
q_l	Problematic line element

Sets:

Ω_N	Distribution system nodes
Ω_L	Distribution system lines
Ω_C	Distribution system clusters
Ω_Z	Distribution system zones
Ω_k	Distribution system FSPs
Ω_{N_z}	Zone buses
Ω_G	Distribution system elements
Ω_Q	Distribution system problematic elements
Ω_{Q_n}	Distribution system problematic nodes
Ω_{Q_l}	Distribution system problematic branches

Parameters and Constants:

C	Number of clusters.
$C_{min/max}$	Minimum. and maximum C
L	Number of branches
N	Number of nodes
$V_n^{max/min}$	Maximum/minimum voltage at node *n*
$V_{gel}^{max/min}$	Maximum/minimum voltage at grid element *gel*
$V_{q_b}^{max/min}$	Maximum/minimum voltage at problematic bus element q_b
V_{q_b}	Voltage at problematic bus element q_b
$I_{q_l}^{max}$	Maximum current at problematic line q_l
I_{q_l}	Current in the problematic line q_l
$I_l^{max/min}$	Maximum and minimum current at branch *l*
$I_{gel}^{max/min}$	Maximum and minimum current at grid element *gel*
I_l^{old}	Current in branch *l* before flexibility variation
V_n^{old}	Voltage in *n* before active power flexibility variation
Z	Number of zones
N_z	Number of nodes in zone z.
G	Number of nodes and branches elements
$Q_n^{max/min}$	Number of problematic node elements (over/under voltage)
Q_l^{max}	Number of problematic branches (over loading)
K	Number of FSP in distribution grid
$u_k^{up/dw}$	Upward/downward bid price of FSP k
C^{β}	Penalty coefficients for $\beta_l^{max^*/min^*}$
C^{α}	Penalty coefficients for $\alpha_n^{max^*/min^*}$
V_b	Base voltage
I_b	Base current
$d(i,n)$	Distance function between nodes *i* and *n*
W_{gel}	Weight function of grid elements
τ	loading percentage parameter

Variables:

$V_n^{re/im}$	Real/imaginary part of the voltage in node n
$X_{i,j}^{re/im}$	Real/imaginary part of the derivative voltage in node i due to active power variation in node j
$I_{ij}^{re/im}$	Real/imaginary part of the current between nodes i and j
$J_{ij,n}^{(re/im)}$	Real/imaginary part of the derivative current between nodes i and j due to active power variation in node n
Y_{ij}	Admittance value between node *i* and *j*
SV	Voltage sensitivity indices matrix
SI	Current sensitivity indices matrix
SV^T	Transposed of SV
SI^T	Transposed of SI
S	Horizontally merged matrix of SV^T SI^T
$SV_{i,j}$	Voltage sensitivity indices at node *i* to power variation at node *j*
$SI_{ij,n}$	Current sensitivity indices between nodes *i* and *j* to power variation at node *n*
SV_{norm}	Normalized voltage sensitivity indices matrix of SV^T
SI_{norm}	Normalized current sensitivity indices matrix of SI^T
$S_{n,z_{vb}}^{v}$	Voltage sensitivity index at node *n* to power variation in the virtual bus of zone *z*
$S_{l,z_{vb}}^{i}$	Current sensitivity index at branch *l* to power variation in the virtual bus of zone *z*
SVI_{norm}	Normalized voltage and current sensitivity indices
$SVI_{norm_{i,gel}}$	Normalized voltage and current sensitivity indices (of node i and grid element *gel*)
ΔP_j	Active power variation in node *j*
ΔP_z	Active power variation in zone *z*
P_j^{vb}	Active power in node *j* considering virtual bus flexibility amount
$\Delta P_j^{up/dw}$	Upward/downward/ available active power in node *j*

$\Delta P_j^{max/min}$	Maximum/minimum available active power in node j
$\Delta P_z^{up/dw}$	Upward/downward available active power flexibility in zone z
$\Delta P_z^{max/min}$	Maximum/minimum available active power flexibility in zone z
ΔP_j^*	Cleared active power flexibility amount at node j
ΔP_z^*	Cleared active power flexibility amount at zone z
ΔP_z^m	Metered active power flexibility amount at zone z
ΔV_n	Voltage variation in node n due to active power variation.
ΔI_l	Current variation in branch l due to active power variation
V_n^{new}	Voltage value in node n after active power variation
I_l^{new}	Current value in branch l after active power variation
$\alpha_n^{max/min}$	Slack variable w.r.t $V_n^{max/min}$
$\beta_l^{max/min}$	Slack variable w.r.t $I_l^{max/min}$
$\alpha_n^{max^*/min^*}$	Flexibility amount not provided to maintain voltage nodes lower than V_n^{max}, or higher than V_n^{min}
$\beta_l^{max^*/min^*}$	Flexibility amount not provided to maintain current branches lower than I_l^{max}
$\lambda^P{}_{LFM}$	Local flexibility market price
$\lambda^P{}_{VoLL}$	Value of Lost Load (VoLL) price
CR_k^{FSP}	Collection revenues for FSP k
PO_k^{FSP}	Penalty obligation for FSP k
NP_k^{FSP}	Net profit for FSP k
DSO_{NC}	DSO net costs
SC_P	Cost of non-served flexibility
$RVSCT_c^{v,i}$	Voltage and current percentage error error regarding cluster arrangement C

Abbreviations

DSO	Distribution system operator
TSO	Transmission system operator
DER	Distributed energy resources
ASM	Active system management
ACER	EU Agency for the Cooperation of Energy Regulators
LFM	Local flexibility market
LMO	Local market operator
IMO	Independent market operator
PA	Product attributes
DA	Day-ahead
ID	Intra-day
OPF	Optimal power flow
RS	Relative sensitivity
SLP	Successive Linear Programming
AOF	Activation Optimization Function
BRP	Balance responsible party
SESP	Smart Energy Service Provider
MILP	Mixed Integer Linear Programming
PN	Pilot node
HC	Hierarchical clustering
SCC	Short-circuit capability
CS	Control sensitivity
AZD	Average zone distance
ROPF	Reactive optimum power flow
HCSD	Hierarchical clustering with single distance
HCVS	Hierarchical clustering VAR control space
SKW	Spectral k-way
FCM	Fuzzy C-means
RD	Relative diameter
AICD	Average inter-cluster distance
Eg	Eigengap
MD	Minimum distance
CAO	Cluster autonomous optimization
DICCO	Distributed inter-cluster coordination optimization
CPI	Cluster performance index
ADN	Active Distribution Network
DESS	Distributed energy storage system
MBC	Model-based control
BESS	Battery energy storage systems
LP VSC	Linear programming with voltage sensitivity indices
VOP	Voltage optimization problem
LPF	Linear power flow equations
VCZ	Voltage control zones
ADMM	Alternating direction method of multipliers
ISP	Imbalance settlement period
GCT	Gate closure time
MDA	Metered data administrator
AT	Austria
BE	Belgium
DE	Germany
LU	Luxemburg
NL	Netherlands
FSPs	Flexible service providers

1 INTRODUCTION AND MOTIVATION

The increasing presence of flexible distributed energy resources (DER), along with supportive regulatory frameworks, is encouraging network customers to actively manage their energy usage by leveraging their flexibility. This enables them to play a key role in integrating variable renewable energy resources by providing flexibility to various stakeholders [1], including distribution and transmission system operators (DSOs and TSOs, respectively). The ability of DSOs and TSOs to utilize DER flexibility makes their coordination crucial for ensuring its efficient use. Thus, regardless of the specific solutions adopted, effective coordination between them is necessary. TSO-DSO coordination mechanisms [1]-[2] aim to establish these coordinated procedures to unlock distributed flexibility for the optimal operation of both TSO and DSO grids. While Article 32 of the EU Directive 2019/944 on common rules for the internal electricity market [3] obliges Member States to establish regulations prompting DSOs to use DER flexibility, Article 182 of the EU Commission Regulation 2017/1485 [4] focuses on TSO-DSO cooperation, ensuring that DER can also provide services to TSOs. The joint ENTSO-E and E.DSO report on active system management (ASM) [5] proposed coordination mechanisms for congestion management and balancing services. These mechanisms are similar to those initially discussed in [2] and were further adopted in the OneNet project [6]. At the end of 2023, ENTSO-E and EU DSO Entity released a draft proposal for the Network Code on Demand Response, and in May 2024, they submitted the proposal to the European Union Agency for the Cooperation of Energy Regulators (ACER) [7]. In view of the above, it is clear that there is a need for further research into the design of flexibility solutions for system operators' services/needs, as well as into the coordination of TSOs and DSOs to ensure the efficient use of distributed resources. In developing these solutions, various market frameworks, optimization methods, and management system models have been proposed.

This paper proposes an intra-day local flexibility market (LFM) based on grid zones. Grid zones allow the local DSO to publish the flexibility needs per zone, allowing flexibility aggregation and clearing per zone. Grid zones are built by the local DSO by grouping grid buses where the activation of flexibility has a similar impact on those grid elements where the constraints are either violated or close to being violated, and are represented with virtual buses (or fictitious nodes [8]). Each virtual bus is then defined by its sensitivities that quantify the average impact of activating flexibility in the buses of the zone it represents on the grid elements with constraints violated or close to being violated. In addition, grid computations are based on sensitivity coefficients [9] that allow to approximate power flows with a linear approach, where the sensitivity coefficients are the linearized impact of activating flexibility in a grid bus on each bus voltage or line current of the grid. Market clearing is performed by minimizing the total cost of the selected flexibility, considering all zones simultaneously and their collective impact on the grid elements where constraints are either violated or close to being violated. The clearing process is not conducted sequentially by zone; instead, it evaluates all flexibility zones in parallel to ensure that existing constraints are addressed without introducing new ones. The impact of the bids from each

flexibility zone is captured through its corresponding virtual bus, which reflects the voltage and current variations across all buses and lines when flexibility is activated.

While market clearing methods rooted in optimal power flow (OPF) [10] are mathematically sound, they require the full grid topology, a detailed characterization of its components, and all active and reactive power values at the grid buses. In contrast, our proposal shares limited strategic information and data with the local market operator (LMO), specifically, how buses are grouped into zones, the sensitivities of virtual buses and the flexibility needs per zone, so that the LMO can apply a simple linear optimization algorithm to clear the market without requiring strategic grid information that DSOs are reluctant to provide.

2 LITERATURE REVIEW

To support the development of the proposed LFM, a systematic review of existing literature was conducted, focusing on two key areas: (1) market-based flexibility solutions and (2) grid segmentation (zone-based) methodologies. This review is summarized in Table 1, which is divided into market and grid segmentation topics, each with its own subtopics. In the market category, the subtopics are type of market (Type), definition of product attributes (PAs), market operator (Operator), market clearing method (Clearing), grid constraints (Grid Const), and flexibility zones (Zones). In grid segmentation, the subtopics are sensitivity indices (Sens. Ind.), zone methodology (Zone method), pilot node (PN), cluster validation (Clust. Valid.) and optimization problem (Opt. Prob.). The grid issue is the last topic, common to both the market and grid segmentation categories.

2.1 Market-based flexibility solutions

As can be seen, most of the identified flexibility market-based solutions are either day-ahead (DA) or intra-day (ID) local markets. In [11], the authors propose a conceptual day-ahead LFM design for congestion management, operated by an independent market operator (IMO). This design defines flexibility needs in terms of product attributes (PAs), such as bid resolution, duration, and activation time. Sensitivity indices are employed to calculate the DSO's flexibility needs; however, the optimization problem for determining these needs is not provided. The sensitivity indices also delineate the flexibility needs zone through a relative sensitivity (RS) parameter, which specifies the relationship between a congested area and a flexibility needs zone. For example, an RS of 100 enables participation from the entire grid, while an RS of zero restricts participation to only the bus experiencing over/under-voltage. However, this methodology defines only a single zone for flexibility activation, and no computational simulations are provided to demonstrate its performance.

In [12], another day-ahead LFM is proposed, targeting congestion management and voltage control services. This work focuses on a Successive Linear Programming (SLP) algorithm, a linear OPF methodology, used for market clearing in the distribution grid. Unlike [11], this design does not include product attributes, sensitivity indices, or flexibility zones. The role of the market operator is not specified

in this work, leaving it unclear whether the market would be operated by the DSO or an independent market operator (IMO). A comparison between SLP and nonlinear OPF algorithms shows that SLP achieves faster solutions with high accuracy across different grid topologies and loading scenarios.

For ID markets, [13] outlines a framework for DSO-TSO market-based coordination. In this framework, the TSO operates a balancing market, while the DSO operates a flexibility market that runs in parallel with the TSO market. Sequential market clearing is proposed, so that the DSO market clears first and forwards the results to the TSO's balancing market, which clears the market through the Activation Optimization Function (AOF) using Common Merit Order Lists as inputs (this is the optimization module of Manual Activated Reserves Initiative platform [14]). In this setup, the DSO acts as a balance responsible party (BRP), submitting offers based on its flexibility market results to maintain the system in balance. While product attributes are discussed, grid constraints, flexibility zones, and market clearing formulation are not addressed. A simple case study illustrates the framework, but it does not include mathematical grid constraints, such as voltage limits at all buses and current limits in all lines. The congestion constraint is included in the Common Merit Order Lists, merged with upward/downward energy demands for the DSO (DSO needs of increasing or decreasing active power activation). In [15], the authors propose an LFM for short-term scheduling of flexible resources via the Smart Energy Service Provider (SESP) platform, involving aggregators, BRPs, and the DSO. The SESP is a market platform provider, that receives flexibility offers and requests. The LFM aligns with the Traffic Light Concept [16], in which a "yellow light" indicates anticipated grid issues. The SESP selects the cheapest flexible resources in the "yellow light" to restore the grid condition to "green light" (grid with no issues). This LFM is modelled using a Mixed Integer Linear Programming (MILP), detailing DER operational constraints but omitting grid constraints related to voltage at the buses and current in the lines. A small case study validates the operation of the platform. The market design does not describe the product attributes, sensitivity indices, or flexibility zones, nor does the study provide grid topology.

In contrast to these short-term markets, EcoGrid 2.0 [17] demonstrates the use of flexibility in a long-term LFM, with products traded from one to twelve months in advance. Operated by an IMO, this market provides two DSO services: capacity limitation and baseline flexibility services for congestion mitigation. The former imposes total power consumption caps on an aggregator's portfolio, while the latter involves load increases or reductions using a predefined baseline as a reference. Some product attributes (PA) are defined, and the market clearing follows the mathematical formulation in [18]. A real medium-voltage feeder with twelve buses is used to validate the services.

2.2 Grid segmentation methods

Grid segmentation involves methodologies for dividing a transmission/distribution network into flexibility zones designed to facilitate the activation of flexibility for voltage and overloading. These zones are typically derived from the network's Jacobian matrix [19]. Each zone is represented by a PN [8], which should be selected so that its voltage and current variations effectively represent the overall

voltage and current dynamics within the zone. In [20], the authors propose an automatic voltage control scheme for secondary and tertiary voltage control in transmission grids, utilizing an adaptive zones division approach. Unlike fixed zones, these control zones are reconfigured online and updated dynamically to adapt to the evolving grid structure and operation. The adaptive zones division relies on sensitivity indices for voltage with respect to reactive power (VAR control space) and transforms the grid segmentation into a clustering problem in a higher-dimensional Euclidean space. This problem is addressed using hierarchical clustering (HC). Once the zones are defined, PNs are selected based on two criteria: short-circuit capability (SCC) and control sensitivity (CS). The number of zones is optimized based on the average zone distance (AZD), which measures the average distance between the members of each zone. Optimal voltage values for the PN in each zone are then computed via reactive optimal power flow (ROPF), which minimizes transmission losses while respecting grid constraints. A real-world application in China demonstrates the effectiveness of this adaptive zone computation for automatic voltage control.

Further research into voltage control in transmission systems is presented in [21], which explores zoning methodologies for an adaptive reduced control model in coordinated voltage regulation. The study evaluates various segmentation techniques, including hierarchical clustering with single distance (HCSD), hierarchical clustering in the VAR control space (HCVS), spectral k-way (SKW), and fuzzy C-means (FCM). Each methodology employs a specific clustering validation metric: HCSD uses the relative diameter (RD), HCVS employs the average inter-cluster distance (AICD), SKW uses the Eigengap (Eg), and FCM relies on the Xie-Beni index [22].

PN selection is based on the minimum distance (MD) criterion within a zone. The research highlights the importance of investigating different grid segmentation methodologies, as they apply varying proximity measurements (sensitivity indices), clustering criteria, and validation indices. A generic framework is proposed to evaluate the performance of coordinated voltage regulation, enabling a comparative analysis of grid segmentation methodologies. This framework incorporates full AC power flow equations and probabilistic analysis to assess their effectiveness.

Grid segmentation methodologies are also applied to distribution networks in [23], [24], [25], [26], [19], and [27]. In [23], the authors propose a double-layer voltage control strategy based on distribution network partitioning. This strategy combines the cluster autonomous optimization (CAO) and distributed inter-cluster coordination optimization (DICCO), operating at different time scales. The CAO refers to autonomous optimization of voltage control within individual zones of a distribution grid. Each zone operates independently to optimize the voltage at the buses using localized resources. DICCO manages the coordination of voltage control across multiple zones and ensures that independent optimization within each zone (via CAO) aligns with the overall network's operational goals. A cluster performance index (CPI), incorporating electrical distance and regional voltage regulation capability, is proposed for segmenting a distribution network into multiple clusters. The optimal number of zones is determined using the Tabu search algorithm applied to the CPI. Instead of traditional OPF, grid

constraints are modelled using LinDistFlow and the alternating direction method of multipliers. The feasibility of the proposed method is demonstrated through simulations on the IEEE 123-bus system and in a real 10.5 kV feeder in China.

In [24] and [25], the authors present network segmentation strategies for optimal voltage control of Active Distribution Networks (ADNs). Specifically, [24] focuses on a decentralized control algorithm using a distributed energy storage system (DESS), while [25] introduces a decentralized model-based control (MBC) framework that relies on dynamic representations of battery energy storage systems (BESS). Both works use segmentation approaches based on linear programming with voltage sensitivity coefficients (LP VSC) to divide the ADN into zones. Each zone is controlled by a single DESS/BESS, ensuring a significant influence on co-zonal node voltages compared to nodes outside the zone. Communication between zones is facilitated by a multi-agent system, in which zones share active and reactive power limits with neighbours. In [24], decentralized control algorithms based on Thevenin and recursive top-down sweep (TDS) approaches are validated on IEEE 13 and 123-bus systems. Since each DESS/BESS has an associated zone, there is no metric to determine the optimal number of zones.

In [26], a centralized control approach is employed within zones to determine the set-points of the DERs in the distribution grid. This control is achieved by solving a voltage optimization problem (VOP) subject to linear power flow equations (LPF) and network constraints. Zones are computed based on sensitivity indices using the voltage control zones (VCZ) methodology. Pilot nodes are identified through an algorithm that considers the node density concept within zones. A low-voltage grid with 24 nodes is used to validate the VOP and benchmark its performance. In [19], the work is expanded with a method for determining the optimal number of zones using the silhouette index, along with an analysis of the impact of the R/X ratio on zone evaluation and VOP outcomes.

In [27], voltage optimization is addressed in two stages. First, grid zones and pilot nodes are computed. Then, the zones are used to optimize voltage profiles using a two-time-scale coordinated approach. Initially, a slow time-scale optimization is performed using linearized power flow equations to determine the set points for the on-load tap changers, step-voltage regulators, and capacitor banks. Second, a fast time-scale optimization is implemented using the alternating direction method of multipliers (ADMM). This step optimizes the voltage at the pilot nodes within each zone by adjusting active and reactive power from DERs. Limited data exchange between pilot nodes ensures that the local optimizations converge to the global system optimum.

2.3 Research contributions

Table 1 summarises the outcome from the literature review, by also highlighting the existing gaps and contributions of our proposed LFM.

Table 1 - Literature review regarding flexibility market-based solutions and grid segmentation methods

ref	Market						Grid segmentation					Grid issue
	Type	PA	Operator	Clearing	Grid. Const	Zones	Sens. Ind.	Zone method	PN	Clust. Valid.	Opt. Prob.	
[11]	DA	✓	IMO			✓	V/P	RS				VC
[12]	DA		IMO|DSO	SLP OPF	✓							CM & VC
[13]	ID	✓	DSO	AOF								
[15]	DA/ID		SESP	MILP								
[17]	LT	✓	IMO	MILP								CM
[20]							V/Q	HC	SCC & CS	AZD	ROPF	VC
[21]								HCSD HCVS SKC FCM	MD	RD AICD Eg Xie and Beni index	OPF	
[23]					✓		V/P	CPI		CPI & Tabu seach	CAO DICCO	
[24]							V/P V/Q	LP VSC			TDS TB	
[25]					✓						MBC	CM & VC
[26]					✓			VCZ	VCZ nodes density	Silhouette	VOP With LPF	VC
[19]					✓							
[27]					✓						VOP With LPF + ADMM	

According to Table 1, the main research gaps identified in the methodologies applied to LFM are:

- LFMs are typically not operated within zones defined by the segmentation of the distribution grid. However, as we demonstrate in this work, clustering techniques and adapted electrical distances can be used to group buses into zones, enabling the aggregation of flexibility. This

approach limits the information that DSOs need to share with the LMO and facilitates aggregation.

- Among the segmentation approaches reviewed, we propose adapting the electrical distance for the segmentation purposes of the LFM, ignoring the impact on grid elements far from their operational limits. This adaptation allows for the computation of larger flexibility zones, simplifying the LFM operation. Additionally, worst-case sensitivity index matrices of the PN, which represent each zone, are crucial in helping DSOs balance a reasonable number of zones with the performance error of the flexibility activation in the buses of the zone. This balance can have significant implications for constraints solving when the flexibility is activated.

Therefore, the main contributions of the approach proposed in this paper are:

- A comprehensive flexibility-zones-based LFM design that outlines all key steps, from computing grid flexibility zones and needs to activating flexibility in order to resolve grid constraints. The DSO computes the flexibility zones and shares them with the LMO, which runs the LFM.
- The LFM zones are computed using an innovative grid segmentation methodology based on [28], which can be easily implemented in DSO systems. This methodology groups buses with a similar impact on the grid elements where constraints are either violated or close to being violated, allowing aggregators to optimize their portfolios per zone.
- The introduction of grid zones and virtual buses within the LFM framework allows the DSO to limit the strategic information and data shared with the LMO, while still ensuring an efficient market-clearing process that accounts for grid constraints.

The remainder of this paper is organized as follows: Section 3 describes the conceptual LFM; Section 4 presents the case study and numerical results for the Cigré MV grid; Section 5 discusses the feasibility, trade-offs, and limitations of zone-based LFMs; and Section 6 highlights the conclusions and directions for future research.

3 CONCEPTUAL LOCAL FLEXIBILITY MARKET

3.1 Market Design Framework

The proposed LFM is based on the theoretical market framework (TMF) presented in [6], as it provides a comprehensive and structured foundation for developing local flexibility markets. This framework helps to ensure that all relevant dimensions and features are systematically considered. The TMF has been applied and validated in real-world demonstrators, such as the OneNet project, providing further evidence of its practical feasibility and relevance.

The theoretical market framework consists of five key pillars: market architecture, sub-market coordination, market optimization, market operation, and grid constraint representation. Each pillar is

further defined by a set of attributes. The market architecture encompasses the features of sub-markets, services, products, location, and market roles and actors. The LFM operates as an auction-based sub-market. According to [29], a sub-market is assumed to be operated by a single market operator, who is responsible for clearing this market according to a specific objective. Therefore, the LFM is operated by an LMO, which clears the LFM to resolve voltage issues and overloading by activating active power flexibility bids. While the DSO and LMO tasks may appear technically similar, their separation is mandated by EU regulations (Directive 2019/944, Article 35) [3] to ensure unbundling, non-discrimination, and market fairness. The DSO's primary role as a grid operator could lead to conflicts of interest if it were to directly administer market operations, especially in cases where grid ownership and commercial energy activities overlap. The LMO's role as an independent entity ensures compliance with cybersecurity, transparency, and equal treatment of participants (Network Code, Article 41) [7], which are critical for market credibility. To align with these principles, several European flexibility markets have adopted independent operators. For instance, Piclo operates flexibility markets in the UK, Portugal, Scandinavian countries, among others [30]. Moreover, NODES has been deployed as an independent market operator in multiple EU projects across countries such as Norway, Sweden, Spain, Greece, and Switzerland [31]. Similarly, Germany's Enera project was operated by EPEX SPOT, which organized flexibility procurement across 23 local market areas. These examples underscore the policy rationale for institutional independence as a design solution for market credibility and promoting economic efficiency. Thus, while the DSO retains a crucial role as the grid operator, assigning market operation to an independent LMO ensures compliance with regulatory requirements to support the transparent and non-discriminatory market design.

The market design employs a 30-minute gate closure time (GCT) with 15-minute imbalance settlement periods (ISPs), aligning with the temporal resolution of EU balancing markets (e.g., mFRR). The 40-minute market opening (allowing 10 minutes for bid submission) follows operational paradigms seen in European intraday markets - notably in Belgium, France, Germany and the Netherlands, where 30-minute GCTs with 1-hour market periods are standard practice [32]. While early gate closure times may allow for significant deviations between real and forecasts data, it is also common for DSO to have day-ahead operation with minor adjustment close to real time based on real time monitoring. In addition, approaches can be found, for example in [33], that mitigate uncertainty impact by using deep learning methods for 1-hour-ahead predictions.

The locational granularity is defined by the grid zones, which are computed dynamically through segmentation, as explained in section 3.2 The DSO acts as the sole buyer, while flexibility service providers (FSPs) or aggregators serve as the sellers. FSPs can voluntarily provide flexibility through (distributed) generators, loads, and storage systems, and they may aggregate the energy offered per zone. In our market design, FSPs are considered to be BRPs, meaning they are responsible for the imbalances of their own portfolios in the wholesale market. This approach aligns with one of the proposals in [34], which explores how aggregators interact with other market actors—such as suppliers and BRPs—under

various regulatory frameworks. The paper proposes six distinct organizational setups and discusses the benefits and limitations of each. By assuming that FSPs also act as BRPs in our design, we streamline responsibility allocation and avoid the need for separate balance reconciliation mechanisms. The metered data administrator (MDA) is responsible for measuring the actual flexibility delivered.

The market optimization pillar [6] refers to the strategies for enhancing market efficiency and minimize flexibility activation costs. In the proposed LFM, optimization is centrally performed by the LMO, with market sessions optimized sequentially for each ISP. The objective of market optimization is to resolve expected grid constraints while minimizing flexibility activation costs.

The LFM operates on a pay-as-bid auction basis, establishing distinct zonal prices for each 15-minute interval (ISP). In this framework, the DSO—acting as the sole buyer—remunerates all cleared active power bids at their respective zonal prices. When multiple zones are cleared, this results in multiple market prices, reflecting localized supply-demand conditions. By differentiating prices across zones, the LFM creates targeted economic incentives for flexibility providers to invest in grid areas where it is most needed. This granular pricing approach enhances the efficiency of grid operations and maintenance.

The current design focuses on zonal flexibility procurement without explicit representation of the power exchange at the TSO-DSO connection point, assuming a negligible impact of DSO flexibility activation in TSO balancing. In practice, very often the flexibility activated by DSOs are indeed negligible for TSO balancing issues, considering, for example, that manual balancing reserve bids must offer more than 1 MW to participate in such markets [35]. If not, however, the DSO could either communicate the flexibility activated to the TSO (which would imply the need for defining a sharing cost mechanism to compensate the TSO for the flexibility activated for balancing), or activate itself additional energy in the opposite sense to keep the system balanced.

Finally, the grid constraint representation pillar [6] refers to how grid constraints are considered in the market framework. In the proposed LFM, grid constraints are addressed using a linearized network constraint based on sensitivities, which minimizes flexibility activation costs subject to the grid constraints. Flexibility needs and bids are defined for each grid zone. In market clearing, the sensitivities of the virtual bus (which represents a grid zone) are used to quantify voltage and current variations due to flexibility activation, ensuring that the market is cleared in a way that respects voltage limits across all nodes and current limits across all lines.

3.2 Intra-day local flexibility market

The proposed LFM operates as an intraday market. A brief review of this type of market is provided in [36]. It follows the concept of the EPEX SPOT intraday 15-minutes auction [37]. The EPEX SPOT intraday market is implemented in Austria (AT), Belgium (BE), Germany (DE) and Luxembourg (LU), and the Netherlands (NL). In these countries, the order books open at 15:00 CET, and the 96 ISPs of the

following day are traded in a single auction [38]. The results are published at 15:10 in DE-LU, at 15:20 in AT, and at 15:40 in BE and NL.

As shown in Figure 1, the proposed LFM has four main phases (dashed rectangles). These phases were defined considering the congestion management market phases in the ASM of [5], the Universal Smart Energy Framework market coordination mechanism phases in [39], and the LFM phases in EUniversal [40]. Figure 1 also presents the main actors, their primary tasks, and their interactions. Each phase is described in detail in the following sections.

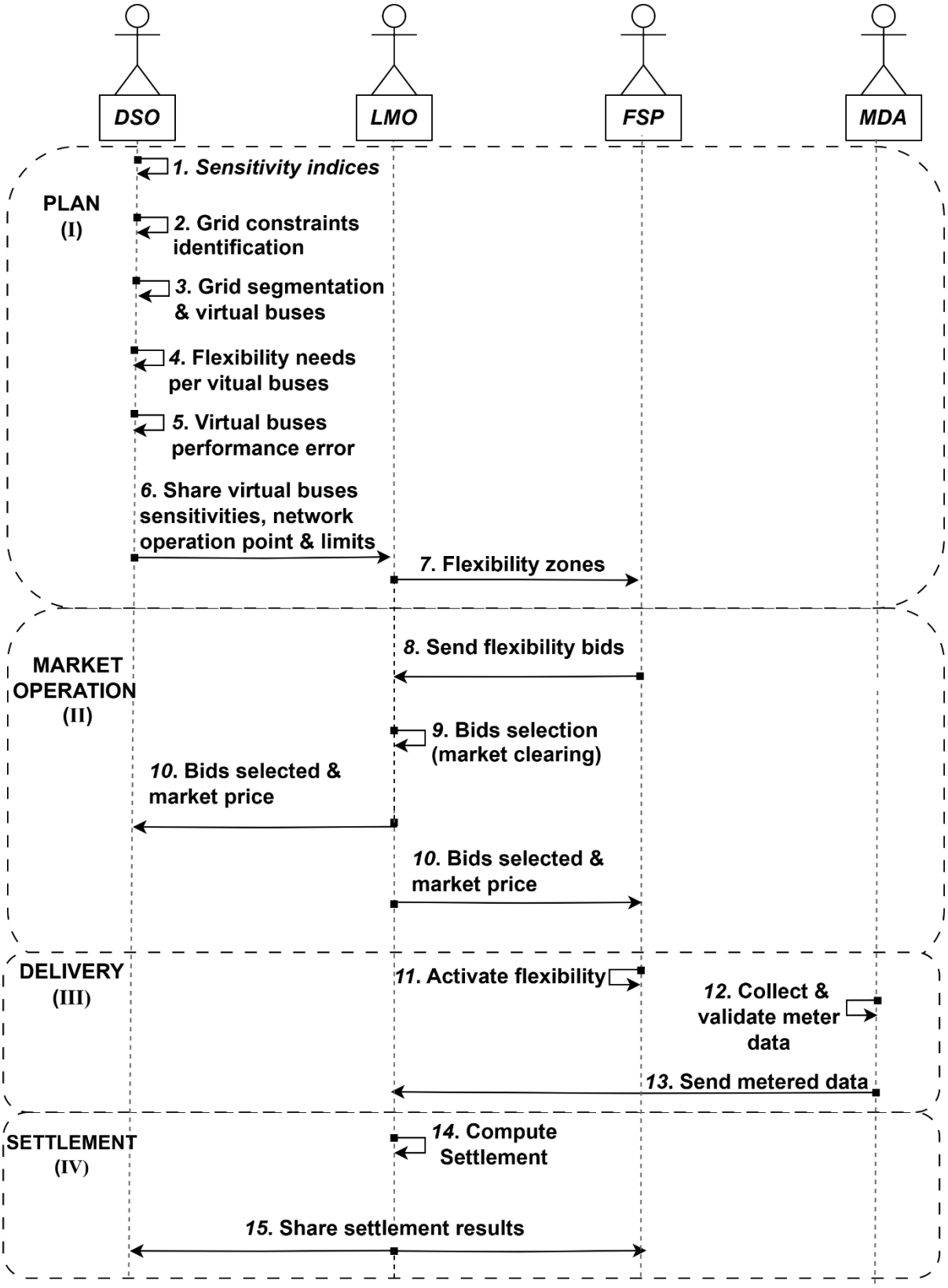

Figure 1 - Sequence diagram of the main stages of the proposed LFM

3.2.1 Plan

The planning phase starts with the computation of the sensitivity indices, derived from the grid topology and the forecasted active and reactive power at the grid buses. Sensitivity indices are used to run a linear power flow analysis to assess potential grid constraint violations. If grid constraints are expected, the sensitivity indices are also used for grid segmentation, and the flexibility zones and flexibility need per zone required to resolve the grid issues are identified.

3.2.1.1 Sensitivity Indices Estimation

The computation of the sensitivity indices is based on the admittance compound matrix method. The sensitivity indices linearly approximate the relationship between a control variable (active power) and a controlled variable (bus voltage or branch current), which depends on the grid topology and operating point (state-dependent). The sensitivity of the voltage magnitude of bus *i,* given the activation of active power flexibility in a bus *j* is defined in(1), and, according to [9], leads to(2).

$$SV_{i,j} = \frac{\partial |V_i|}{\partial P_j} \quad \textbf{(1)}$$

$$SV_{i,j} = \frac{V_i^{re} \times X_{i,j}^{re} + V_i^{im} \times X_{i,j}^{im}}{\sqrt{(V_i^{re})^2 + \left(V_i^{im}\right)^2}} \quad \textbf{(2)}$$

The sensitivity of the current magnitude through a line *ij* when flexibility is activated at bus *n* ((3) can be calculated by multiplying the admittance Y_{ij} by the voltage difference between buses *i* and *j* (4). Equation (5) represents the derivative of(4), and by rewriting the latter, the current sensitivity is given by(6).

$$SI_{ij,n} = \frac{\partial |I_{ij}|}{\partial P_n} \quad \textbf{(3)}$$

$$I_{ij} = Y_{ij} \times \left(V_i - V_j\right) \quad \textbf{(4)}$$

$$J_{ij,n} = \frac{\partial I_{ij}}{\partial P_n} = Y_{ij} \times \left(\frac{\partial V_i}{\partial P_n} - \frac{\partial V_j}{\partial P_n}\right) \quad \textbf{(5)}$$

$$SI_{ij,n} = \frac{I_{ij}^{re} \times J_{ij,n}^{re} + I_{ij}^{im} \times J_{ij,n}^{im}}{\sqrt{\left(I_{ij}^{re}\right)^2 + \left(I_{ij}^{im}\right)^2}} \quad \textbf{(6)}$$

3.2.1.2 Identification of Grid Constraints Violation

To identify grid constraint violations, the DSO computes the flexibility per node that would resolve the anticipated grid issues, using the minimization problem described in equations (7) to (22).

$$\min_{\Delta P_j^{up/dw}, \beta^{max/min}, \alpha^{max/min}} \left[\sum_{J}^{N} \left(\Delta P_j^{up} - \Delta P_j^{dw} \right) + SC_P \right] \quad (7)$$

Where,

$$SC_P = \sum_{l}^{L} C^{\beta} \times \left(|\beta_l^{min^*}| + |\beta_l^{max^*}| \right) + \sum_{n}^{N} C^{\alpha} \times \left(|\alpha_n^{min^*}| + |\alpha_n^{max^*}| \right) \quad (8)$$

Subject to:

$$0 \leq \Delta P_j^{up} \leq \Delta P_j^{max}, \forall j \in \Omega_N, \quad (9)$$

$$\Delta P_j^{min} \leq \Delta P_j^{dw} \leq 0, \forall j \in \Omega_N, \quad (10)$$

$$\Delta V_n = \sum_{n}^{N} \sum_{j}^{N} \left(\Delta P_j^{up} + \Delta P_j^{dw} \right) \times SV_{nj}, \forall j \; \forall n \in \Omega_N \quad (11)$$

$$V_n^{new} = V_n^{old} + \Delta V_n, \forall n \in \Omega_N \quad (12)$$

$$V_n^{min} \leq V_n^{new} + \alpha^{min}{}_n, \forall n \in \Omega_N, \quad (13)$$

$$V_n^{new} - \alpha^{max}{}_n \leq V_n^{max}, \forall n \in \Omega_N \quad (14)$$

$$\alpha_n^{min^*} = \alpha^{min}{}_n \times I_b \times V_b, \forall n \in \Omega_N \quad (15)$$

$$\alpha_n^{max^*} = \alpha^{max}{}_n \times I_b \times V_b, \forall n \in \Omega_N \quad (16)$$

$$\Delta I_l = \sum_{l}^{L} \sum_{j}^{N} \left(\Delta P_j^{up} + \Delta P_j^{dw} \right) \times SI_{lj}, \forall j \in \Omega_N, \forall l \in \Omega_L \quad (17)$$

$$I_l^{new} = I_l^{old} + \Delta I_l, \forall l \in \Omega_L, \quad (18)$$

$$I_l^{min} \leq I_l^{new} + \beta^{min}{}_l, \forall l \in \Omega_L, \quad (19)$$

$$I_l^{new} - \beta^{max}{}_l \leq I_l^{max}, \forall l \in \Omega_L, \quad (20)$$

$$\beta_l^{min^*} = \beta^{min}{}_l \times I_b \times V_b, \forall l \in \Omega_L, \quad (21)$$

$$\beta_l^{max^*} = \beta^{max}{}_l \times I_b \times V_b, \forall l \in \Omega_L. \quad (22)$$

The objective function (7) aims to find the minimum amount of flexibility (either upward or downward) needed to resolve all voltage and current grid issues, and constraints (9) to (22) form a linearized network voltage and current constraints. The second term in the objective function represents the cost of non-served flexibility (SC_P), which is computed in (8). This cost differs from zero either when there is insufficient flexibility to address the anticipated grid issues, or when the sensitivity indices are misaligned, causing flexibility activation based on these indices to fail in resolving the grid issues (the latter can occur with the virtual bus sensitivities, described in 3.2.1.3). Constraints (9) and (10) set the maximum upward and minimum downward flexibility that a resource can provide. Constraints (11) and (17) compute the voltage and current variation in the buses and branches due to active power flexibility, using voltage and current sensitivity indices for each bus and each branch, respectively. The constraints

from (12) to (16) are voltage- related constraints. (12) computes the new voltage value at the bus due to flexibility activation considering the voltage sensitivity indices. The voltage limits in per unit with slack variables for minimum and maximum operational limits are described in (13) and (14). The voltage slack values are converted to MWh in (15) and (16). The constraints from (18) to (22) are current-related constraints. (18) computes the new current value in the branch due to flexibility activation considering the current sensitivity indices. The current limits in per unit with slack variables for minimum and maximum operational limits are described in(19) and (20). The current slack variables are transformed into MWh in (21) and (22).

3.2.1.3 Grid Segmentation and Virtual Buses

The grid segmentation methodology, initially introduced in [28], has been significantly enhanced in this study. Originally designed to divide the distribution grid into zones to address DSO flexibility needs, it now incorporates improvements focusing on two key aspects: the computation of virtual bus indices and the assessment of the performance errors associated with the selected virtual buses. These enhancements improve the methodology's effectiveness in addressing DSO flexibility needs. The methodology encompasses the following steps:

- Compute normalized voltage and current sensitivity indices.
- Apply an ad hoc distance-based on a weighting function that considers how far buses are from each other [28].
- Compute virtual buses, following the approach outlined in [8].
- Evaluate the performance errors resulting from the selected virtual buses.

The normalized voltage and current sensitivity indices are computed according to (23) and (24), respectively. Normalization is performed to transform voltage and current sensitivity indices into comparable indices, by dividing each voltage/current sensitivity matrix by the nominal voltage/current values of the bus or line column in the respective matrix:

$$SV_{norm}[:,i] = \frac{SV^T[:,i]}{V_i} \times 100, \forall i \in \Omega_N, \quad \textbf{(23)}$$

$$SI_{norm}[:,l] = \frac{SI^T[:,l]}{I_l} \times 100, \forall l \in \Omega_L, \quad \textbf{(24)}$$

The next step is to horizontally merge the sensitivity indices matrix, as shown in (25), where each row of the matrix corresponds to a grid bus:

$$SVI_{norm} = [SV_{norm}, SI_{norm}], \forall l \in \Omega_L, \forall n \in \Omega_N \quad \textbf{(25)}$$

After obtaining the complete sensitivity indices matrix in (25), the buses in this matrix (rows) are grouped based on the distance function described in (26) borrowed from [28]. Based on this distance, buses are considered close when activating flexibility in them has a similar impact on the problematic grid elements, defined as buses or branches nearing or surpassing their acceptable operational limits. This distance function computes the difference in normalized sensitivity indices between bus *i* and *n* (rows of the matrix) for each grid element (columns of the matrix) multiplied by a weight function which is computed differently for buses or branches (columns) as shown in (27) and (28). Figure 2 shows the graphical representation of the weight function for the buses (a) and for the lines (b).

$$d(i,n) = \sum_{g_{el}}^{G} W_{gel} \times \left| SVI_{norm_{i,g_{el}}} - SVI_{norm_{n,g_{el}}} \right| \quad \textbf{(26)}$$

$$, \forall n, i \in \Omega_N, \forall\, gel \in \Omega_G$$

$$W_{gel} = \begin{cases} 1, & V_{gel} \geq V_{gel}^{max} \;||\; V_{gel} \leq V_{gel}^{min} \\ 0.1, & V_{gel} = 1\ p.u. \\ \left|1 - V_{gel}\right| \times 10, & V_{gel}^{min} < V_{gel} < V_{gel}^{max} \end{cases} \quad \textbf{(27)}$$

$$W_{gel} = \begin{cases} 1, & I_{gel} \geq I_{gel}^{max} \\ \frac{I_{gel}}{I_{gel}^{max}}, & I_{gel}^{max} \times \tau \leq I_{gel} < I_{gel}^{max} \\ 0, & I_{gel} < I_{gel}^{max} \times \tau \end{cases} \quad \textbf{(28)}$$

As shown in Figure 2(a), the voltage weight function equals one when the voltage at a bus element is either at or above the maximum voltage value or at or below the minimum voltage value. For buses within these limits, the weight function ranges between zero and one. A bus element with a voltage of one p.u. has a voltage weight of zero. This voltage weight affects the distance described in (26). Moreover, for problematic buses, the voltage weight function increases the computed distance.

Similarly, as shown in Figure 2(b), the current weight function is equal to one if the current in a branch element exceeds its maximum value. The parameter $\boldsymbol{\tau}$ represents the overloading percentage of a branch, which is determined by the DSO. For instance, if $\boldsymbol{\tau}$ is set to 80%, then branches operating below this value will have a current weight of zero. If the current falls between 80% and the maximum allowable value, the current weight function will range between zero and one.

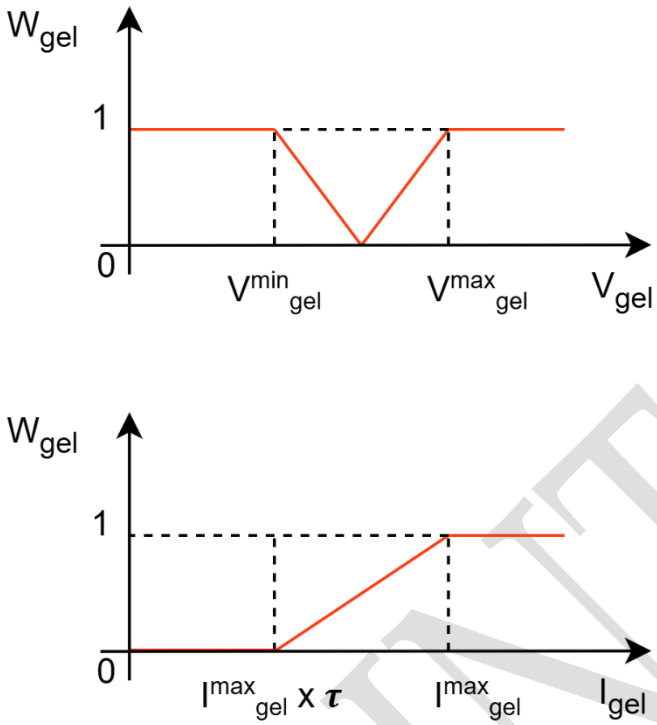

Figure 2 - Graphical representation of the weight function

Given this distance function, clustering procedures can be applied to group buses. The hierarchical clustering algorithm [41], an unsupervised learning algorithm, was selected and applied using the *fclusterdata* function [42] and the distance from (26). For each cluster or zone, its virtual bus is computed using (29) and (30) as an average representation of the zone. In (29), the transposed sensitivity indices matrix for voltage and current is horizontally merged. Using this matrix, along with the index of buses for each zone, the virtual bus of a zone is computed as the average of the sensitivity indices for the buses within that zone.

$$S = [SV^T SI^T] \tag{29}$$

$$z_{vb} = \frac{1}{N_z} \times \sum_{nc}^{N_z} [S_{(nc,:)}] \tag{30}$$

3.2.1.4 Flexibility Needs per Virtual Buses

For each virtual bus, the DSO computes the minimum flexibility needed to solve the anticipated set of grid issues. Using virtual buses allows the DSO to provide simplified and less strategic information to the LMO, for running the LFM, and enables the FSP to optimize their portfolio per zone (tasks 5 and 6 in Figure 1). Flexibility needs are computed using (31) to (37).

$$\min_{\Delta P_z^{up/dw}, \beta^{max/min}, \alpha^{max/min}} \left[\sum_{z}^{N_z} \left(\Delta P_z^{up} - \Delta P_z^{dw} \right) + SC_P \right] \tag{31}$$

Subject to:

$$0 \le \Delta P_z^{up} \le \Delta P_z^{max}, \forall z \in \Omega_Z, \quad \textbf{(32)}$$

$$\Delta P_z^{min} \le \Delta P_z^{dw} \le 0, \forall z \in \Omega_Z, \quad \textbf{(33)}$$

$$\Delta V_n = \sum_{n}^{N} \sum_{z}^{N_z} \left(\Delta P_z^{up} + \Delta P_z^{dw}\right) \times S_{n,z_{vb}}^{v}, \forall n \in \Omega_N, \forall z \in \Omega_Z \quad \textbf{(34)}$$

$$((12) - (16) \quad \textbf{(35)}$$

$$\Delta I_l = \sum_{l}^{L} \sum_{z}^{N_z} \left(\Delta P_z^{up} + \Delta P_z^{dw}\right) \times S_{l,z_{vb}}^{i}, \forall l \in \Omega_L, \forall z \in \Omega_Z, \quad \textbf{(36)}$$

$$((18) - (22) \quad \textbf{(37)}$$

(31) defines the objective function to find the minimum amount of flexibility from the identified zones. Since, at this stage no FSP bids are available, real flexibility costs cannot be considered. Constraints (32) and (33) set the maximum upward and minimum downward flexibility that a zone can provide. Constraints (34) and (36) compute the voltage and current variations in the buses and branches due to active power flexibility using the virtual bus sensitivity indices for each bus and branch, respectively. Constraints (35) and (37) are related to voltage and current values, limits, and slack variables.

As noted, the main difference between this model and the grid constraints identification is the amount of flexibility available (zone-based *versus* bus-based) and the sensitivity indices of virtual buses instead of those of buses and lines.

3.2.1.5 Virtual Buses Performance Error

The virtual buses performance error (step 5 in Figure 1) is the last task in the planning phase, where the DSO checks whether the activation of this flexibility at the buses of the zone can effectively solve the grid issues. Therefore, for each node *j* of the virtual bus *vb*, the voltage and current at the nodes and lines of the grid are computed by considering the buses' sensitivities and the virtual bus flexibility amount, as described in (42) and (43) for voltage, and (44) and (45) for current.

$$\Delta V_n = \sum_{n}^{N} \left(P_j^{vb}\right) \times SV_{nj}, \forall j \in \Omega_{N_z}, \forall n \in \Omega_N \quad \textbf{(38)}$$

$$V_n^{new} = V_n^{old} + \Delta V_n, \forall n \in \Omega_N \quad \textbf{(39)}$$

$$\Delta I_l = \sum_{l}^{L} \left(P_j^{vb}\right) \times SI_{lj}, \forall j \in \Omega_{N_z}, \forall l \in \Omega_L \quad \textbf{(40)}$$

$$I_l^{new} = I_l^{old} + \Delta I_l, \forall l \in \Omega_L, \quad \textbf{(41)}$$

The voltage and current values, after activating the virtual bus flexibility at each bus of the zone represented by the virtual bus in equations ((43) and (45), are compared with the limit values of nodes

and branches to check if the grid issues have been solved. If they are not solved, the performance error is computed using (46) and (47), and the bus with the highest performance error determined by ((48), defines the performance error of the virtual bus.

$$RVSCT_c^v = \left[\sum_{q_b}^{Q_n{}^{max}} \frac{\left(V_{q_b} - V_{q_b}^{max}\right)}{V_{q_b}^{max}} + \sum_{q_b}^{Q_n{}^{min}} \frac{\left(V_{q_b}^{min} - V_{q_b}\right)}{V_{q_b}^{min}}\right] \times 100 \quad \textbf{(42)}$$

$$RVSCT_c^i = \sum_{q_l}^{Q_l{}^{max}} \frac{\left(I_{q_l} - I_{q_l}^{max}\right)}{I_{q_l}^{max}} \quad \textbf{(43)}$$

$$RVSCT_c^{v,i} = [RVSCT_c^v, RVSCT_c^i] \quad \textbf{(44)}$$

3.2.2 Market Operation

The market operation phase starts when the FSPs submit their flexibility bids to the LMO (task 8 in Figure 1). Note that if the baseline is based on the *Meter-Before-Meter-After* (see section 3.2.3) the submission of the baselines is not strictly needed. Flexibility bids must be submitted to the LMO before the GCT (30 minutes before delivery). After the GCT, the LMO clears the market (task 9 in Figure 1) using equations (45) and (46) to minimize the cost of the activated flexibility.

$$\min_{\Delta P_z^{up/dw}, \beta^{max/min}, \alpha^{max/min}} \left[\sum_z^{N_z} \left(u_k^{up} \times \Delta P_z^{up} - u_k^{dw} \times \Delta P_z^{dw}\right) + SC_P\right] \quad \textbf{(45)}$$

Subject to:

$$((32) - (37)) \quad \textbf{(46)}$$

The first part of (45) aims to minimize the cost of flexibility activation (either upward or downward) to solve the grid issues. The second part introduces a penalty (cost of non-served flexibility) in cases where there is insufficient flexibility in the zones to solve the anticipated grid issues. Therefore, whenever the slack variables in (13), (14), (19) and (20) are nonzero, costs associated with non-served flexibility arise. The penalty coefficients C^{β}, C^{α} can be determined by the regulatory authority, as seen in the case of the Single Intraday Coupling in Spain [43]. In this study, the penalty coefficients were taken from the report Estimation of the Value of Lost Load in Europe, by ACER [44]. Thus, C^{β}, C^{α} correspond to the Spanish annual average of Value of Lost of Load (VoLL), which is 7.88 (€/kWh).

3.2.3 Delivery and Settlement

After the LMO clears the market, the selected bids are sent to the DSO (task 10 in Figure 1) and to the FSPs. At this stage, the DSO may decide whether or not to activate the awarded flexibility based on real-time operational needs. However, the financial settlement of the flexibility service is based on the market clearing outcome, FSPs are remunerated for cleared bids regardless of whether the service is ultimately activated. This preserves the integrity and transparency of the market while ensuring that the DSO maintains operational control.

To verify the flexibility provided by FSPs (task 11 in Figure 1), the MDA collects the metered data from the FSPs' resources and sends it to the LMO (tasks12 and 13 in Figure 1) to compute the settlement. While the LMO clears the market, it is still common that activation and settlement fall in the side of the DSO [45]. However, we propose that the final settlement is done by the LMO by aggregating the market clearing results with the flexibility provision verification from the metered data. In this sense, when the activated flexibility is not fully delivered, a penalty may be applied.

The scientific literature presents different baseline methods and their pros and cons. For example, see [46] for the PJM case or [47] for the EU case. We assume that the method *Meter-Before-Meter-After* can be the best option for near real-time products, according to the findings in [48]. In this method, a meter reading is conducted immediately before the flexibility activation (meter before, MB), establishing the baseline, and another reading is taken immediately after flexibility activation (meter after, MA), serving as the final setpoint. The delivered flexibility is computed as the difference between the readings. Accordingly, the LMO computes, for each FSP:

- Revenue collection from the selected and committed flexibility (47).
- Penalty obligations due the non-compliance with the commitment (48).
- Net profit calculated using (49).

The LMO also calculates the DSO's net costs (task 14 in Figure 1) using (50). Finally, the LMO shares the settlement results with the FSPs and the DSO (task 15 in Figure 1).

$$CR_k^{FSP} = \Delta P_z^{*} \times \lambda^{P}{}_{LFM} \quad \textbf{(47)}$$

$$PO_k^{FSP} = |\Delta P_z^{*} - \Delta P_z^{m}| \times \lambda^{P}{}_{VoLL} \quad \textbf{(48)}$$

$$NP_k^{FSP} = CR_k^{FSP} - PO_k^{FSP} \quad \textbf{(49)}$$

$$DSO_{NC} = \left(\sum_{k}^{K} NP_k^{FSP} \right) \quad \textbf{(50)}$$

1

4 CASE STUDY AND RESULTS

The European 20 kV Cigré MV network benchmark [49] is used as a case study. The network topology consists of two feeders; however, only Feeder 1 is used since the main load and flexibility resources are located there. Moreover, all switches are open, resulting in a radial topology. Figure 3 shows the grid topology, including the location of loads and DERs, as well as the identification numbers of the buses and lines. The DER units and the loads are described in Table 2 and Table 3**Error! Reference source not found.** respectively. While the physical characteristics of the DER units and loads are represented within the grid topology, we do not develop mathematical models for the different types of resources. This is because the proposed market design aims to be technology agnostic. As such, unless specific bidding rules are required for certain resource types—which is not the approach adopted in this work—the detailed modelling and management of individual resources are left to the responsibility of the aggregators or FSPs, who are expected to ensure that the committed flexibility can be delivered.

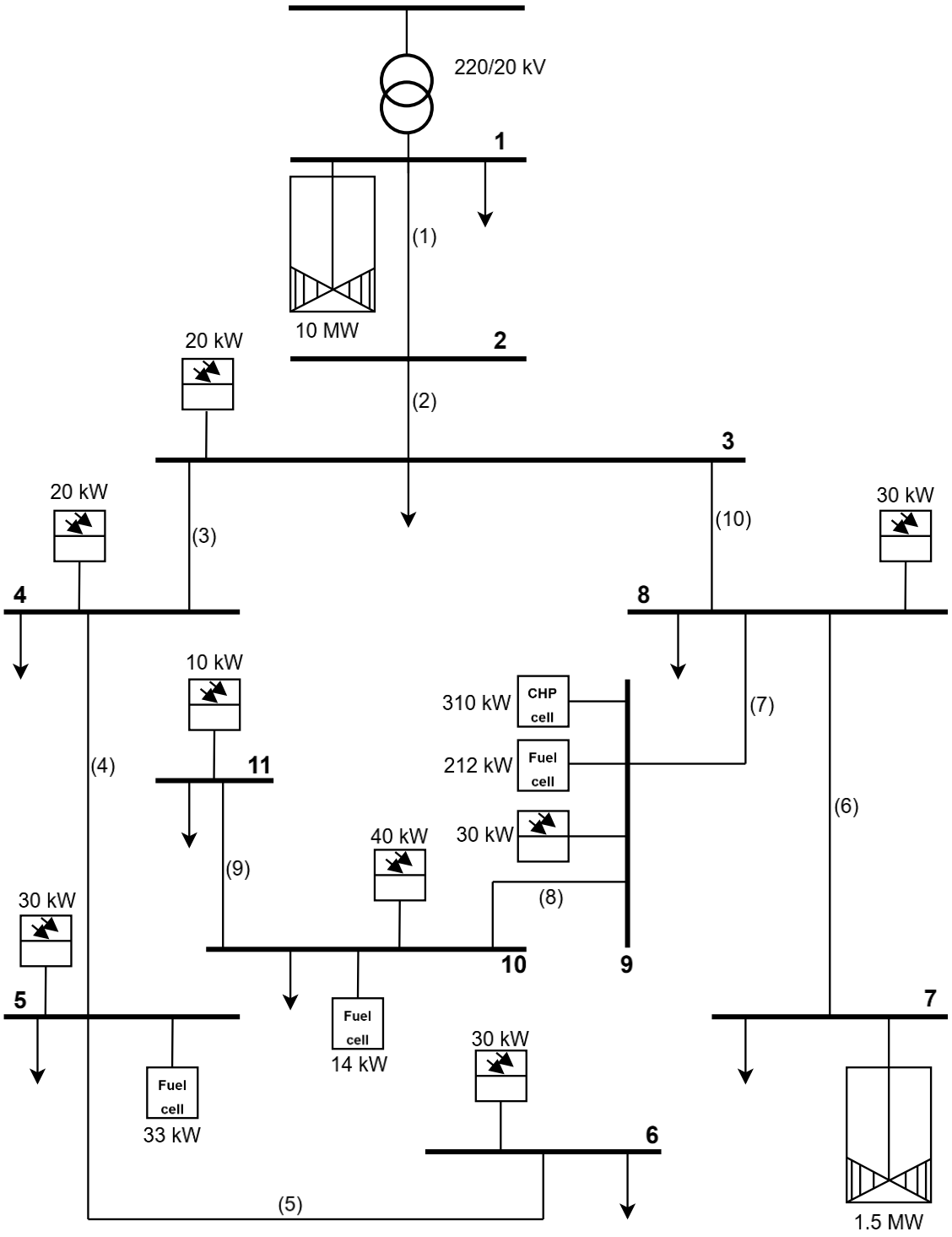

Figure 3 – Revised European Cigré MV distribution network with DERs [50]

Table 2 - MV distribution network benchmark DER resources example

Node	DER type	Pmax
1	Wind turbines	30 MW
3	PV	23 kW
4	PV	20 kW
5	PV	30 kW
5	Residential fuel cell	33 kW
6	PV	30 kW
7	Wind turbine	1.5 MW
8	PV	30 kW
9	PV	30 kW
9	CHP DIESEL	310 kW
9	Fuel cell	212 kW
10	PV	40 kW
11	PV	10 kW

Table 3 - Load parameters of European MW example

Node	Load	P_MW	Q:MVAR	Sn_MVA
1	Load R1	0	0	10
3	Load R3	0	0	0.285
4	Load R4	0	0	0.445
5	Load R5	0	0	0.750
6	Load R6	0	1	10
8	Load R8	0	0	0.605
10	Load R10	0	0	0.490
11	Load R11	1	0	1.4
1	Load CI1	0	0	5.1
3	Load CI3	0	1	0.265
7	Load CI7	1	1	10
6	Load CI6	1	0	10

All grid-related data are provided in [50] and the voltage and current forecast for a specific timestamp are depicted in Figure 4 and Figure 5, respectively (v and i) as black curves, with the operational limits represented by red dashed lines (1.05 p.u. for voltage and 116 Ampère for lines). As observed, bus 1 experiences overvoltage, while branches 1 and 2 are overloaded. Therefore, the DSO needs upward flexibility, either from demand response or increased generation. Figure 4 and Figure 5 also show the voltage and current values after the flexibility activation, where each colour corresponds to a different number of zones: green for three zones (c3), dark blue for 4 (c4), pink for 6 (c6), and cyan for 8 (c8).

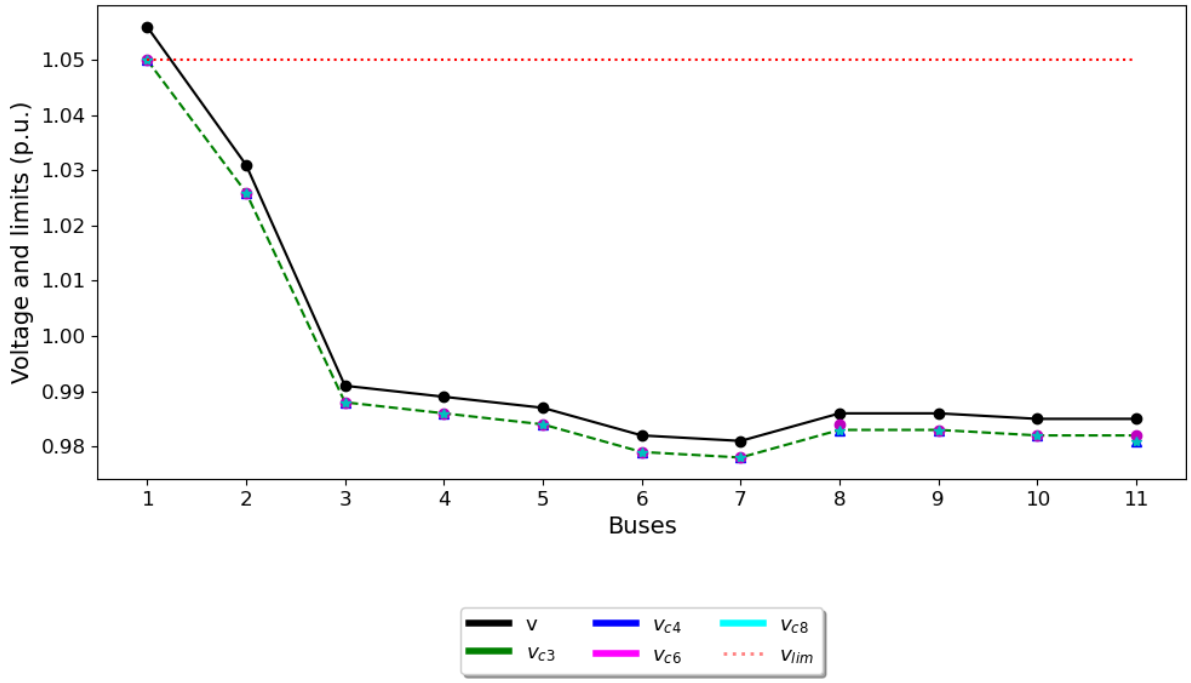

Figure 4 - Voltage values and limits before and after flexibility activation

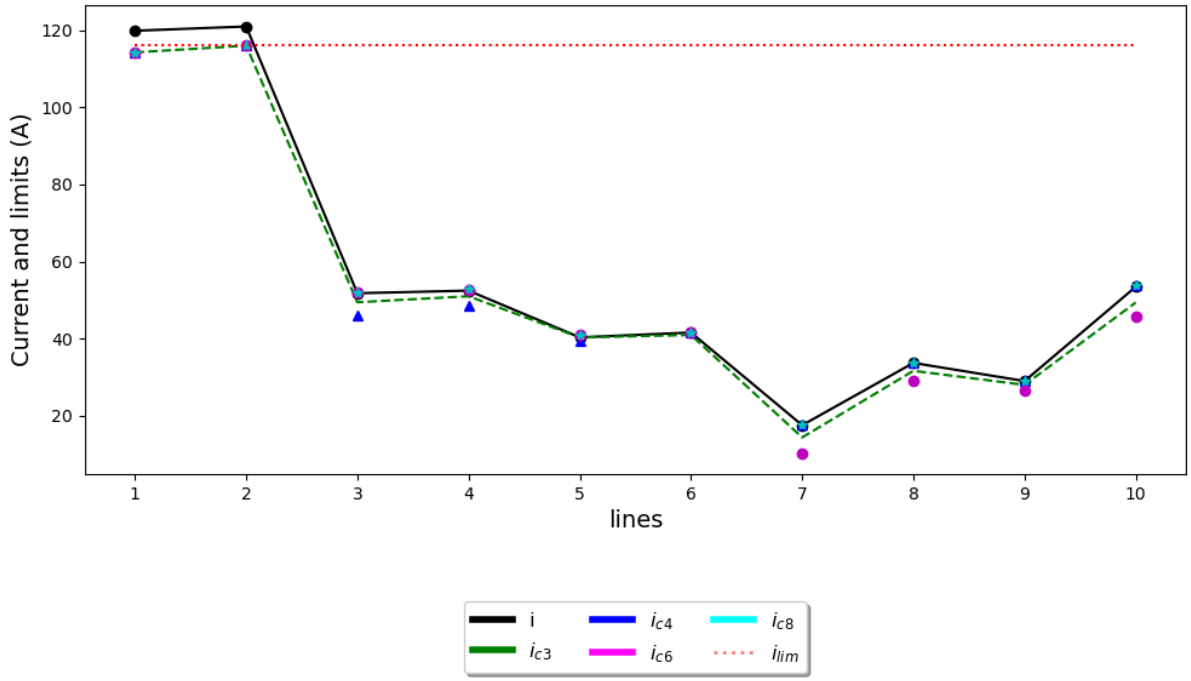

Figure 5 - Current values and limits before and after flexibility activation

The available flexibility per bus and its price are depicted in Figure 6, following the bus numbering from Figure 3. Figure 6 presents (a) buses where the flexibility magnitude is in the order of magnitude of megawatt-hours (MWh) (buses 1, 6, and 7) and in (b) buses where the magnitude is in kilowatt-hours (kWh) (buses 3, 4, 5, 8, 9, 10 and 11). Flexibility prices were set based on the average and standard deviation of prices from the first session on 01/26/2024 [51] in the Spanish intraday auction market.

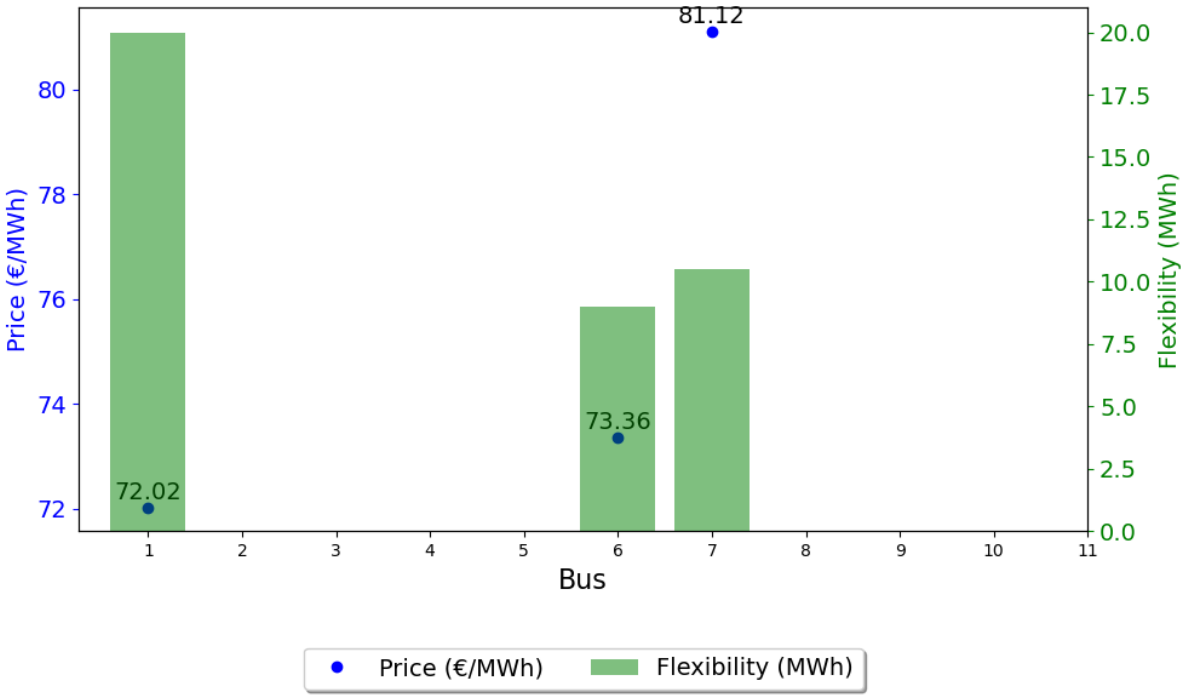

(a) Buses 1, 6 and 7

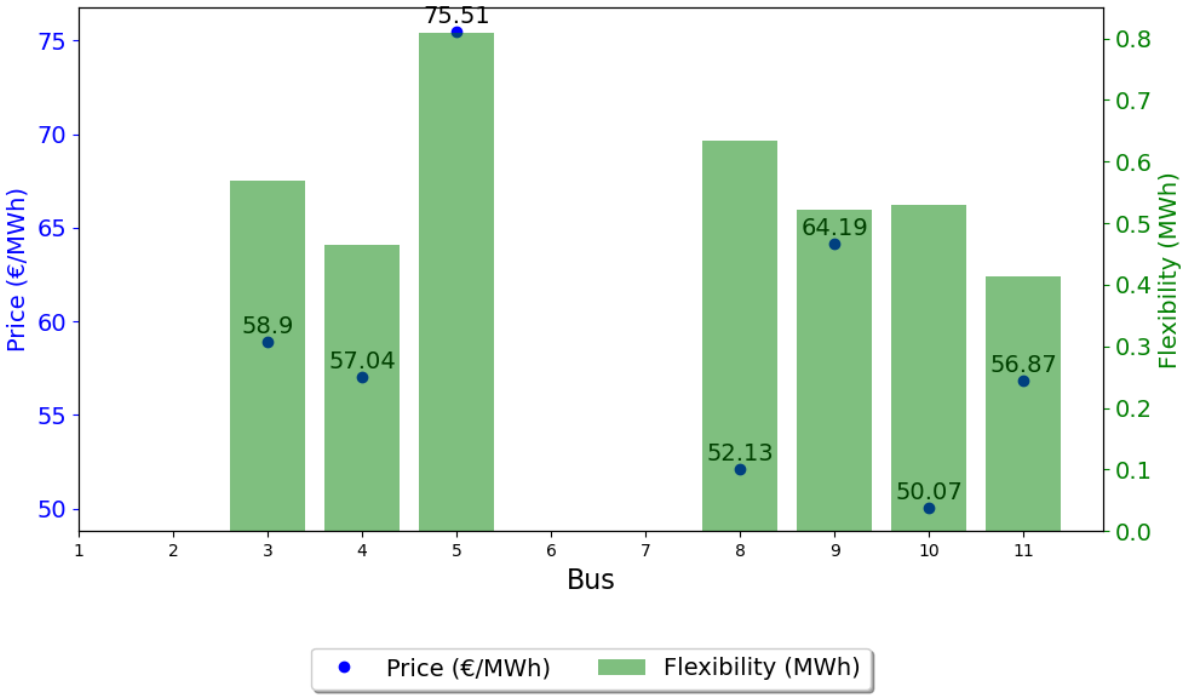

(b) Buses, 3, 4, 5, 8, 9, 10, 11

Figure 6 - Available flexibility and its price

The grid segmentation results for the selected grid are summarized in Table 4, showing the breakdown of buses per zone for each number of zones tested (from two to ten zones, given the size of the test grid).

The same results were obtained for nine and ten clusters, so the last column of Table 4 illustrates the buses in the zones for both cases. For each number of zones defined in the LFM, the buses are assigned to specific zones. The notation Z1, refers to Zone 1, Z2, to zone 2 and so on. Thus, a bus listed under Z1 (Zone 1) belongs to that specific zone. For clarity, each zone is assigned a distinct colour to visually identify its associated buses.

Table 4 - Grid segmentation results for 2 to 10 zones

Buses	**Number of zones**							
	2	***3***	***4***	***5***	***6***	***7***	***8***	***9(10)***
1	Z2	Z2	Z3	Z4	Z5	Z6	Z7	Z8
2	Z2	Z3	Z4	Z5	Z6	Z7	Z8	Z9
3	Z1	Z1	Z1	Z1	Z1	Z2	Z2	Z3
4	Z1	Z1	Z1	Z1	Z1	Z1	Z1	Z1
5	Z1	Z1	Z1	Z1	Z1	Z1	Z1	Z2
6	Z1	Z1	Z1	Z1	Z2	Z3	Z3	Z4
7	Z1	Z1	Z2	Z3	Z4	Z5	Z6	Z7
8	Z1	Z1	Z2	Z2	Z3	Z4	Z5	Z6
9	Z1	Z1	Z2	Z2	Z3	Z4	Z5	Z6
10	Z1	Z1	Z2	Z2	Z3	Z4	Z4	Z5
11	Z1	Z1	Z2	Z2	Z3	Z4	Z4	Z5

Figure 7 shows the amount of cleared flexibility per zone depending on the number of zones, as well as the total costs associated with flexibility provision (DSO net cost plus non-served flexibility), which are displayed in red above each column. Non-served flexibility occurs only for 2 zones. Detailed results are provided in Table 6 of the Appendix.

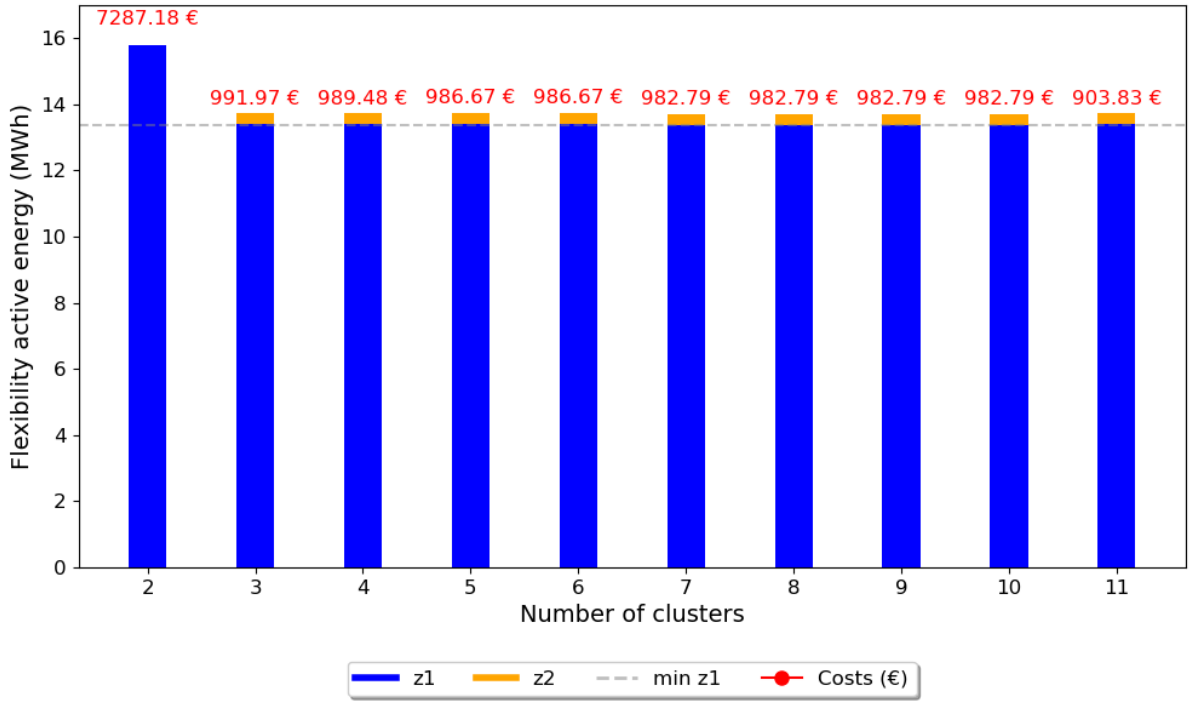

Figure 7 - Cleared flexibility in LFM

As shown in Figure 7, the maximum cost occurs for a two-zone segmentation, even though only one zone (z1) provides the flexibility. This cost is higher due to a lack of sufficient flexibility and the corresponding cost of non-served flexibility. It is important to note that the flexibility and liquidity are the same in all cluster arrangement since the same bids are considered in all cases. Therefore, the cost of non-served flexibility occurs because the flexibility activation in the virtual buses with only two zones does not solve the grid issues.

Starting from three zones and beyond, flexibility is always activated in two zones. However, these two zones are not always the same, as shown in Table 4. The minimum DSO net costs are associated with having either seven, eight, nine, or ten zones. When each bus is treated as a zone, the DSO net costs are €903.83.

Finally, Table 5 shows the virtual buses performance error (section 3.2.1.5) as a function of the number of zones. In our example, voltage and current percentage errors mainly occur for a two-zone segmentation. Beyond three zones, there are no voltage errors, only current errors. From three to ten zones, the current percentage error is around 10%. With eleven zones (each bus a zone), neither voltage

nor current errors are present. Therefore, the DSO must choose a threshold error in order to select the number of zones.

Table 5 -Virtual buses performance error

Number of zones	$RVSCT_c^v(\%)$	$RVSCT_c^i(\%)$
2	3.16	81.57
3	0	11.62
4	0	11.57
5-6	0	11.55
7-8	0	11.53
9-10	0	11.53
11	0	0

Since the segmentation methodology uses a linear power flow approximation based on the sensitivity indices, a relevant question that arises is how the results of this linear model compare to those obtained from the nonlinear power flow model. To assess the impact on the grid voltages, Figure 8 presents the voltage values at each bus for the activation of each flexibility zone computed using the nonlinear power flow equations. For each segmentation configuration, the flexibility cleared in the LFM was applied with a simulated nonlinear power flow model to evaluate whether the flexibility determined by the linear model was sufficient to resolve the grid constraints under a more accurate nonlinear analysis. In Figure 8, the vertical axis represents the number of flexibility zones considered in the LFM, while the horizontal axis corresponds to the bus index of the grid (as numbered in Figure 3). According to Table 6, the amount of cleared flexibility is identical for the following pairs of zone configurations: five and six, seven and eight, and nine and ten. Therefore, these pairs are grouped together on the vertical axis of Figure 8.

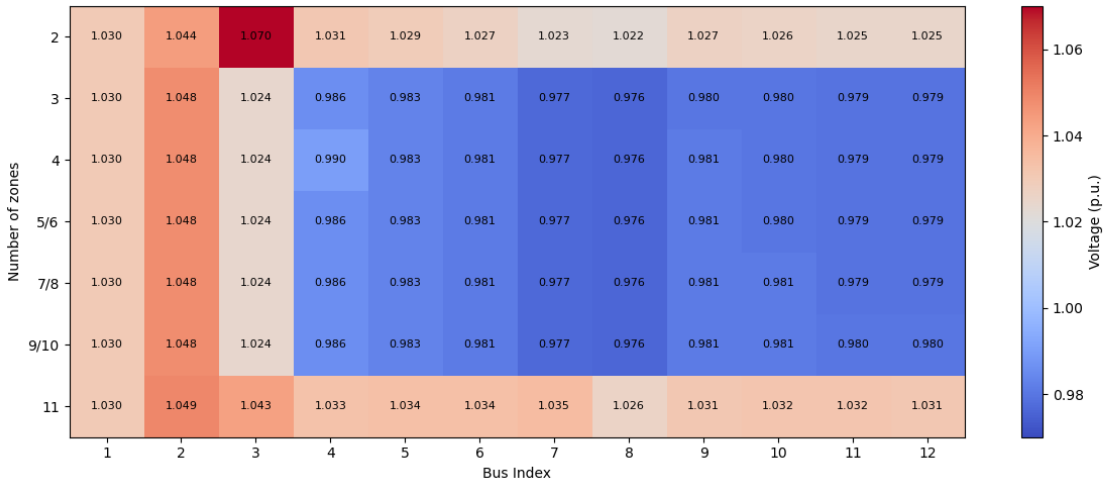

Figure 8 - Voltage values considering flexibility activation through nonlinear power flow

As shown in Figure 8, when only two flexibility zones are considered, the grid still experiences overvoltage at bus 3. This result is consistent with the data in Table 6**Error! Reference source not**

found. (for two clusters), which indicates that with just two zones, it is not possible to provide all the flexibility needed to solve the grid issues, resulting in a cost of non-served flexibility. From three zones onward, the flexibility activated using the linear approach is sufficient to mitigate voltage violations, even when results are computed with the nonlinear power flow model, highlighting the benefits of increased segmentation granularity. Similarly, Figure 9 shows the grid lines currents for each flexibility zone configuration, computed with the nonlinear power flow equations. In this figure, the vertical axis indicates the number of flexibility zones considered in the LFM, while the horizontal axis represents the grid line index.

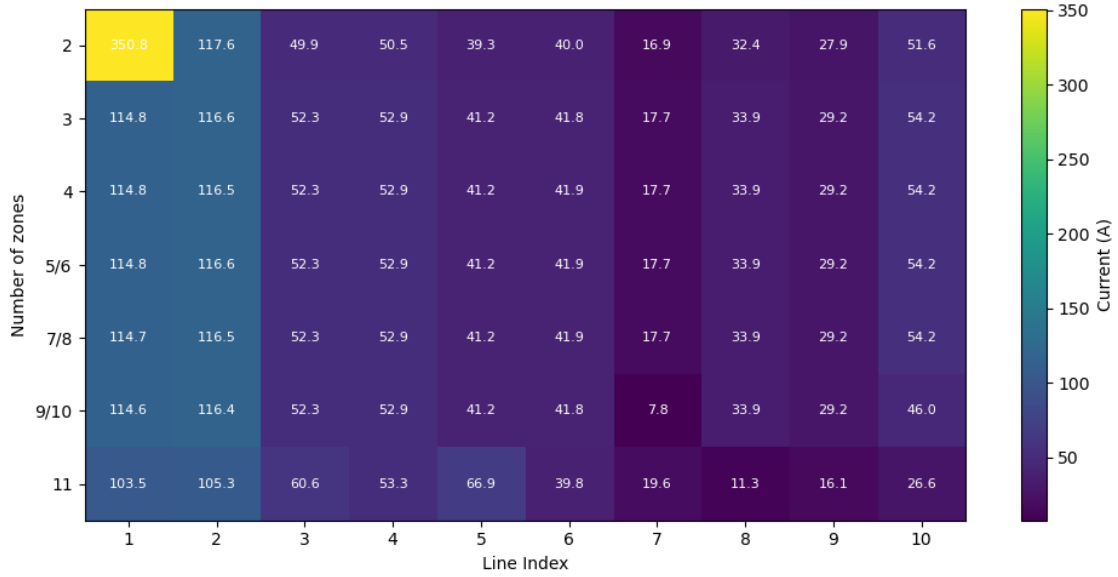

Figure 9 - Current values considering flexibility activation through nonlinear power flow

Figure 9 shows the results of activating the flexibility computed with the linear LFM when using the nonlinear power flow. As can be seen, when only two zones are considered, the grid still experiences overloads in lines 1 and 2. This result aligns with Table 6**Error! Reference source not found.** data (for two clusters), where the limited zonal segmentation fails to provide enough flexibility to solve the grid constraints, resulting in a cost of non-served flexibility. From three to ten zones, the amount of activated flexibility appears enough to mitigate the overloads, as the current in line 2 slightly exceeds its limit by only 0.5%. When each bus is treated as an individual zone, all line currents remain below their respective limits, confirming again that finer segmentation leads to more accurate and effective flexibility dispatch, but increases computational complexity and data exchanged between the DSO and the LMO.

5 DISCUSSION

Based on the outcomes of the case study some benefits and limitations of the methodology can be observed:

- Solving voltage and overloading problems through flexibility zones seems feasible and cost-effective. Indeed, constraints can be solved with a limited number of zones with a cost very close to the minimum cost that would occur if no zones are considered (around 8%). The feasibility of the zones-based LFM was verified in the proposed case study, by analysing the impact on the grid constraints of the activation of the flexibility cleared using the nonlinear power flow equations.

- Using virtual buses allows the DSO to provide simplified and less information to the LMO. This simplified information is sufficient for the LMO to clear the market while accounting for grid constraints, avoiding the need to merely generate a merit order list and delegate the technical selection of flexibility to the DSO, a process that may raise regulatory concerns related to unbundling.

- The error in virtual bus performance streamlines the effectiveness of solving grid issues through the grid segmentation methodology, since beyond three clusters the error is around to 10%. This error helps can also be used to decide the number of zones for optimal market performance considering the trade-off between the error and the computation and use of a larger number of zones. Nevertheless, as already explained, this error does not represent the real error of activating flexibility when considering nonlinear power flow model, which we discuss below.

- One potential drawback could be the DSO's cost for solving the grid constraints based on the defined zones. Although clustering helps manage the complexity of the problem, adding more zones does not always translate into a proportional reduction in the cost of solving grid constraints—especially since this relationship can vary depending on the clustering method applied. However, it is possible to increase the number of zones to identify when the cost stabilizes, or compare it with the cost of solving the constraints at bus level, to have a cost reference for solving the grid constraints. Thus, combining this with the error allows for the assessment of a reasonable range for the number of zones.

- Linear sensitivities of bus voltages and line currents may also be a limitation of the approach. In the case study developed, it was verified that activating the flexibility cleared in zonal LFM based on the linear approach was enough to solve grid issues even when computing their impact with the nonlinear power flow. Indeed, depending on the specific grid and on the operating point where the linearization is applied, the amount of flexibility activation could lead to infeasible

or inaccurate results. However, the market-clearing algorithm is intended for operational planning or near-real-time flexibility scheduling, where system deviations from the nominal operating point are generally moderate, supporting the validity of the linear approximation.

- This work does not account for inaccurate baselines or DSO forecasts. Discrepancies between FSP baselines and DSO forecasts do not compromise the market design, and the role of the baselines is solely to validate the flexibility delivered by the FSP. However, inaccurate estimations represent real challenges faced by FSPs and DSOs. Ultimately, what matters most to the DSO is to maintain well-calibrated and effective forecasting procedures, regardless of how closely they align with FSP baselines.

6 CONCLUSIONS

This paper proposes an intraday LFM, which operates based on grid segmentation. FSPs offer active power flexibility for both voltage control and overloading services to the DSO. The main contribution is a comprehensive dynamic grid segmentation methodology that divides the distribution grid into zones. The zones allow the DSO to assess the flexibility needs per zone and provide limited but strategic information to the LMO, enabling it to clear the market while considering grid constraints, and allowing FSPs to aggregate their resources by zones. This methodology was tested in the European 20 kV Cigré MV network benchmark, and the results showed that: a) it is possible to solve voltage control and overloading issues through zones at costs similar to solving these issues disaggregated per node, b) clearing the market with virtual buses enables the achievement of feasible solutions with low errors, provided that virtual buses performance is used to determine the optimal number of zones, and, c) the DSO's choice of the number of zones should rely not only on costs, but also on virtual bus performance.

Some topics for future work should encompass the limitations of this paper, such as the distance function used to group buses. As mentioned before, the DSO cost does not always decrease with the number of zones. Thus, another methodology can be developed to address this limitation. Moreover, this work does not consider the possible limited duration of flexibility delivery by providers compared to the service duration requested by the DSO. Therefore, technical and operational constraints of flexibility resources can be added to the proposed methodology in order to tackle this limitation.

Another limitation of the market design is that the proposed approach does not yet include distributed renewable energy sources in TSO markets. However, a TSO-DSO coordination methodology should be developed based on the harmonization of products and a bid-forwarding methodology to transfer the unused flexibility bids from the LFM to a TSO balancing market, such as Manual Frequency Restoration Reserve, ensuring that TSO activated flexibility does not jeopardize distribution system operational limits. In this case, a settlement scheme must be designed to account for the provision of flexibility services to different system operators simultaneously. Moreover, the concept of zones has potential for further development by exploring different methodologies for grouping buses, such as using fuzzy

systems instead of deterministic methods in the distance function. Future work should also focus on developing static grid zones based on past operation data, considering, for instance, data-driven approaches.

7 ACKNOWLEDGEMENTS

This research was funded by the Portuguese Foundation for Science and Technology (FCT) under the grant UI/BD/152277/2021.

8 REFERENCES

[1] R. Amaral Lopes, R. Grønborg Junker, J. Martins, J. Murta-Pina, G. Reynders, and H. Madsen, "Characterisation and use of energy flexibility in water pumping and storage systems," *Appl. Energy*, vol. 277, p. 115587, Nov. 2020, doi: 10.1016/j.apenergy.2020.115587.

[2] SmartNet consortium, "SmartNet: TSO-DSO Coordination for Acquiring Ancillary Services from Distribution Grids," no. May 2019, [Online]. Available: http://smartnet-project.eu/wp-content/uploads/2019/05/SmartNet-Booktlet.pdf.

[3] E. Commission, "Directive (EU) 2019/944 of the European Parliament and of the Council of 5 June 2019 on common rules for the internal market for electricity and amending Directive 2012/27/EU," 2019. [Online]. Available: http://data.europa.eu/eli/dir/2019/944/oj/eng.

[4] E. Union, "Commission Regulation (EU) 2017/1485 of 2 August 2017 establishing a guideline on electricity transmission system operation." [Online]. Available: https://eur-lex.europa.eu/legal-content/EN/TXT/?uri=uriserv:OJ.L_.2017.220.01.0001.01.ENG&toc=OJ:L:2017:220:TOC.

[5] G. CEDEC, E.DSO, ENTSO-E, Eurelectric, "No TSO-DSO Report: An Integrated Approach to Active System Management," 2019, [Online]. Available: https://eur-lex.europa.eu/legal-content/EN/TXT/?uri=uriserv:OJ.L_.2017.220.01.0001.01.ENG&toc=OJ:L:2017:220:TOC.

[6] M. Troncia, J. P. Chaves Ávila, C. Damas Silva, H. Gerard, and G. Willeghems, "Market-Based TSO–DSO Coordination: A Comprehensive Theoretical Market Framework and Lessons from Real-World Implementations," *Energies*, vol. 16, no. 19, p. 6939, Oct. 2023, doi: 10.3390/en16196939.

[7] A. for the C. of E. Regulators, "ACER webinar: draft network code on demand response," 2024. [Online]. Available: https://www.acer.europa.eu/public-events/acer-webinar-draft-network-code-demand-response.

[8] P. Lagonotte, J. C. Sabonnadiere, J.-Y. Leost, and J.-P. Paul, "Structural analysis of the electrical system: application to secondary voltage control in France," *IEEE Trans. Power Syst.*, vol. 4, no. 2, pp. 479–486, May 1989, doi: 10.1109/59.193819.

[9] K. Christakou, J.-Y. LeBoudec, M. Paolone, and D.-C. Tomozei, "Efficient Computation of Sensitivity Coefficients of Node Voltages and Line Currents in Unbalanced Radial Electrical Distribution Networks," *IEEE Trans. Smart Grid*, vol. 4, no. 2, pp. 741–750, Jun. 2013, doi: 10.1109/TSG.2012.2221751.

[10] L. A. Roald, D. Pozo, A. Papavasiliou, D. K. Molzahn, J. Kazempour, and A. Conejo, "Power systems optimization under uncertainty: A review of methods and applications," *Electr. Power Syst. Res.*, vol. 214, p. 108725, Jan. 2023, doi: 10.1016/j.epsr.2022.108725.

[11] M. Attar, S. Repo, F. Gaumnitz, and A. Ulbig, "A proposal for implementing short-term congestion management market in distribution networks," in *2022 IEEE PES Innovative Smart Grid Technologies Conference Europe (ISGT-Europe)*, 2022, pp. 1–5, doi: 10.1109/ISGT-Europe54678.2022.9960591.

[12] G. K. Papazoglou, A. A. Forouli, E. A. Bakirtzis, P. N. Biskas, and A. G. Bakirtzis, "Day-ahead local flexibility market for active and reactive power with linearized network constraints," *Electr. Power Syst. Res.*, vol. 212, p. 108317, Nov. 2022, doi: 10.1016/j.epsr.2022.108317.

[13] S. I. Vagropoulos, P. N. Biskas, and A. G. Bakirtzis, “Market-based TSO-DSO coordination for enhanced flexibility services provision,” *Electr. Power Syst. Res.*, vol. 208, p. 107883, Jul. 2022, doi: 10.1016/j.epsr.2022.107883.

[14] ENTSO-E, “MARI Activation Optimization Function Public Description,” [Online]. Available: https://www.statnett.no/globalassets/for-aktorer-i-kraftsystemet/utvikling-av-kraftsystemet/mari_aof_publicdocumentation_v1.0_sfa.pdf.

[15] P. Olivella-Rosell *et al.*, “Optimization problem for meeting distribution system operator requests in local flexibility markets with distributed energy resources,” *Appl. Energy*, vol. 210, pp. 881–895, Jan. 2018, doi: 10.1016/j.apenergy.2017.08.136.

[16] G. A. of the E. and W. I. (BDEW)., “Discussion paper Smart Grid Traffic Light Concept. Design of the amber phase,” 2015.

[17] C. Heinrich, C. Ziras, A. L. A. Syrri, and H. W. Bindner, “EcoGrid 2.0: A large-scale field trial of a local flexibility market,” *Appl. Energy*, vol. 261, p. 114399, Mar. 2020, doi: 10.1016/j.apenergy.2019.114399.

[18] C. Kok, J. Kazempour, and P. Pinson, “A DSO-Level Contract Market for Conditional Demand Response,” doi: 10.1109/PTC.2019.8810943.

[19] A. R. Di Fazio, M. Russo, and M. De Santis, “Zoning Evaluation for Voltage Optimization in Distribution Networks with Distributed Energy Resources,” *Energies*, vol. 12, no. 3, p. 390, Jan. 2019, doi: 10.3390/en12030390.

[20] H. Sun, Q. Guo, B. Zhang, W. Wu, and B. Wang, “An Adaptive Zone-Division-Based Automatic Voltage Control System With Applications in China,” *IEEE Trans. Power Syst.*, vol. 28, no. 2, pp. 1816–1828, May 2013, doi: 10.1109/TPWRS.2012.2228013.

[21] V. Alimisis and P. C. Taylor, “Zoning Evaluation for Improved Coordinated Automatic Voltage Control,” *IEEE Trans. Power Syst.*, vol. 30, no. 5, pp. 2736–2746, Sep. 2015, doi: 10.1109/TPWRS.2014.2369428.

[22] X. L. Xie and G. Beni, “A validity measure for fuzzy clustering,” *IEEE Trans. Pattern Anal. Mach. Intell.*, vol. 13, no. 8, pp. 841–847, 1991, doi: 10.1109/34.85677.

[23] Y. Chai, L. Guo, C. Wang, Z. Zhao, X. Du, and J. Pan, “Network Partition and Voltage Coordination Control for Distribution Networks With High Penetration of Distributed PV Units,” *IEEE Trans. Power Syst.*, vol. 33, no. 3, pp. 3396–3407, May 2018, doi: 10.1109/TPWRS.2018.2813400.

[24] M. Bahramipanah, R. Cherkaoui, and M. Paolone, “Decentralized voltage control of clustered active distribution network by means of energy storage systems,” *Electr. Power Syst. Res.*, vol. 136, pp. 370–382, Jul. 2016, doi: 10.1016/j.epsr.2016.03.021.

[25] M. Bahramipanah, D. Torregrossa, R. Cherkaoui, and M. Paolone, “A Decentralized Adaptive Model-Based Real-Time Control for Active Distribution Networks Using Battery Energy Storage Systems,” *IEEE Trans. Smart Grid*, vol. 9, no. 4, pp. 3406–3418, Jul. 2018, doi: 10.1109/TSG.2016.2631569.

[26] A. R. Di Fazio, M. Russo, and M. De Santis, “Zoning Evaluation for Voltage Control in Smart Distribution Networks,” in *2018 IEEE International Conference on Environment and Electrical Engineering and 2018 IEEE Industrial and Commercial Power Systems Europe (EEEIC / I&CPS Europe)*, 2018, pp. 1–6, doi:

10.1109/EEEIC.2018.8493761.

[27] A. R. Di Fazio, C. Risi, M. Russo, and M. De Santis, “Coordinated Optimization for Zone-Based Voltage Control in Distribution Grids,” *IEEE Trans. Ind. Appl.*, vol. 58, no. 1, pp. 173–184, Jan. 2022, doi: 10.1109/TIA.2021.3129731.

[28] F. Retorta, C. Gouveia, G. Sampaio, R. Bessa, and J. Villar, “Local flexibility need estimation based on distribution grid segmentation,” in *2022 18th International Conference on the European Energy Market (EEM)*, 2022, pp. 1–6, doi: 10.1109/EEM54602.2022.9920997.

[29] K. K., S. S. Torbaghan, A. Virag, and H. Le Cadre, “D3.2 Magnitude Project-Evaluation of Future Market Designs for Multy Energy System.”

[30] T. Schittekatte and L. Meeus, “Flexibility markets: Q&A with project pioneers,” *Util. Policy*, vol. 63, p. 101017, Apr. 2020, doi: 10.1016/j.jup.2020.101017.

[31] CHONDROGIANNIS Stamatios; VASILJEVSKA Julija; MARINOPOULOS Antonios ; PAPAIOANNOU Ioulia; FLEGO Gianluca, “Local electricity flexibility markets in Europe,” 2022. doi: 10.2760/9977.

[32] T. Brijs, Cedric De Jonghe, Benjamin F. Hobbs, and Ronnie Belmans, “Interactions between the design of short-term electricity markets in the CWE region and power system flexibility,” *Appl. Energy*, vol. 195, no. 36–51, p. 16, 2017, doi: http://doi.org/10.1016/j.apenergy.2017.03.026.

[33] R. Nadimi and Mika Goto, “Uncertainty reduction in power forecasting of virtual power plant: From day-ahead to balancing markets,” *Renew. Energy*, vol. 238, no. 121875, 2025, doi: http://doi.org/10.1016/j.renene.2024.121875.

[34] K. Poplavskaya and L. de Vries, “A (not so) Independent Aggregator in the Balancing Market Theory, Policy and Reality Check,” in *2018 15th International Conference on the European Energy Market (EEM)*, 2018, pp. 1–6, doi: 10.1109/EEM.2018.8469981.

[35] ENTSO-E, “Explanatory document to all TSOs’ proposal for the implementation framework for a European platform for the exchange of balancing energy from frequency restoration reserves with manual activation in accordance with Article 20 of Commission Regulation (EU).” [Online]. Available: https://eepublicdownloads.entsoe.eu/clean-documents/nc-tasks/EBGL/EBGL_A20_181218_ALL TSOs proposal_mFRRIF_explanatory_document_for submission.pdf.

[36] P. Shinde and M. Amelin, “A Literature Review of Intraday Electricity Markets and Prices,” in *2019 IEEE Milan PowerTech*, 2019, pp. 1–6, doi: 10.1109/PTC.2019.8810752.

[37] E. SPOT, “Trading at EPEX SPOT 2021.” [Online]. Available: https://www.epexspot.com/sites/default/files/2021-05/21-03-15_Trading Brochure.pdf.

[38] E. SPOT, “Trading Products.” https://www.epexspot.com/en/tradingproducts#intraday-trading.

[39] USEF, “USEF: The Framework Explained.” [Online]. Available: https://www.usef.energy/app/uploads/2016/12/USEF_TheFrameworkExplained-18nov15.pdf.

[40] J. P. C. Á. et Al, “EUniversal - Deliverable D5.1 - Identification of relevant market mechanisms for the

procurement of flexibility needs and grid services." [Online]. Available: https://euniversal.eu/wp-content/uploads/2021/02/EUniversal_D5.1.pdf.

[41] Scipy, "Hierarchical clustering (scipy.cluster.hierarchy) — SciPy v1.12.0 Manual." https://docs.scipy.org/doc/scipy/reference/cluster.hierarchy.html.

[42] Scipy., "cluster.hierarchy.fclusterdata — SciPy v1.12.0 Manual." https://docs.scipy.org/doc/scipy/reference/generated/scipy.cluster.hierarchy.fclusterdata.html#scipy.cluster.hierarchy.fclusterdata.

[43] M. para la T. E. y el R. Demográfico., "Propuesta de Resolución de la Dirección General de Política Energética y Minas por la que se fijan los valores del valor de carga perdida y el estándar de fiabilidad, de conformidad con lo previsto en el Reglamento (UE) 2019/943 del Parlamento Europeo,." https://www.miteco.gob.es/es/energia/participacion/2023-y-anteriores/detalle-participacion-publica-k-641.html.

[44] C. E. P. A. L. ACER, "Study on the estimation of the values of lost load of electricity supply in Europe." [Online]. Available: https://www.acer.europa.eu/sites/default/files/documents/en/Electricity/Infrastructure_and_network development/Infrastructure/Documents/CEPA study on the Value of Lost Load in the electricity supply.pdf.

[45] R. Bessa *et al.*, "Deliverable D1.2. Framework for a flexibility-centric energy and cross-sector value chain, business use cases and KPI definition," 2024. [Online]. Available: https://beflexible.eu/wp-content/uploads/2024/04/BeFlexible-D1.2-Framework-for-Flexibility-Centric-Energy.pdf.

[46] N. Rossetto, "Measuring the intangible: an overview of the methodologies for calculating customer baseline load in PJM," [Online]. Available: https://fsr.eui.eu/publications/?handle=1814/54744.

[47] V. R. et Al, "ONENET-D3.4. Regulatory and demo assessment of proposed integrated markets," [Online]. Available: https://cadmus.eui.eu/bitstream/handle/1814/76110/RSC_RR_Regulatory_and_demo_assessment_OneNet.pdf?sequence=1&isAllowed=y.

[48] L. Lind, J. P. Chaves-Ávila, O. Valarezo, A. Sanjab, and L. Olmos, "Baseline methods for distributed flexibility in power systems considering resource, market, and product characteristics," *Util. Policy*, vol. 86, p. 101688, Feb. 2024, doi: 10.1016/j.jup.2023.101688.

[49] CIGRE, "Benchmark Systems for Network Integration of Renewable and Distributed Energy Resources," [Online]. Available: https://e-cigre.org/publication/ELT_273_8-benchmark-systems-for-network-integration-of-renewable-and-distributed-energy-resources.

[50] Pandapower, "CIGRE Networks — pandapower 2.13.1 documentation." https://pandapower.readthedocs.io/en/v2.13.1/networks/cigre.html#medium-voltage-distribution-network-with-all-der.

[51] OMIE, "Intraday price Session 1 - 26/01/2024." https://www.omie.es/en/market-results/daily/intradaily-market/intradaily-market-price?scope=daily&date=2024-01-26&session=1.

1

9 Appendix

Table 6: Detailed local flexibility market related data regarding the assessed number of clusters

Number of cluster	Offers (€/MWh, MWh)	Market clearing & prices (€/MWh, MWh)	Settlement (€)	DSO costs (€)
2	u_{z1} = 81.12 : ΔP_{z1} = 129.47 u_{z2} = 72.02 : ΔP_{z2} = 42.24	u_{z2} = 72.02 ΔP_{z2} = 15.808	$z1_{\Omega_N}$ = [0] $z2_{\Omega_N}$=[1138.49] SC_P= 6148.69	7287.18
3	u_{z1} = 81.12 : ΔP_{z1}= 129.47 u_{z2} = 72.02 : ΔP_{z2}= 42.24 u_{z3} = -.- : ΔP_{z3}= 0.0	u_{z1} = 81.12 ΔP_{z1}= 0.329 u_{z1} = 72.02 ΔP_{z2}= 13.403	$z1_{\Omega_N}$ = [26.69] $z2_{\Omega_N}$= [965.28] $z3_{\Omega_N}$= [0]	991.97
4	u_{z1} = 75.51 : ΔP_{z1} = 67.68 u_{z2} = 81.12 : ΔP_{z2} = 61.69 u_{z3} = 72.02 : ΔP_{z3} = 42.24 u_{z4} = -.- : ΔP_{z1} = 0.0	u_{z1} = 75.51 ΔP_{z1}= 0.331 u_{z3} = 72.02 ΔP_{z3}= 13.392	$z1_{\Omega_N}$ = [24.99] $z2_{\Omega_N}$ = [0] $z3_{\Omega_N}$= [964.49] $z4_{\Omega_N}$= [0]	989.48
5	u_{z1} = 75.51 : ΔP_{z1} = 67.68 u_{z2} = 64.12 : ΔP_{z2} = 1.693 u_{z3} = 81.12 : ΔP_{z3} = 60 u_{z4} = 72.02 : ΔP_{z4} = 42.24	u_{z2} = 64.12 ΔP_{z2}= 0.328 u_{z4} = 72.02 ΔP_{z4}= 13.408	$z1_{\Omega_N}$= [0] $z2_{\Omega_N}$=[21.03] $z3_{\Omega_N}$= [0] $z4_{\Omega_N}$= [965.64]	986.67

	u_{z5} = -.- : ΔP_{z5} = 0.0		$z5_{\Omega_N}$= [0]	
	u_{z1} = 75.51 : ΔP_{z1} = 1.15		$z1_{\Omega_N}$= [0]	
	u_{z2} = 73.36 : ΔP_{z2} = 66.63	u_{z3} = 64.12	$z2_{\Omega_N}$= [0]	
	u_{z3} = 64.12 : ΔP_{z3} = 1.693	ΔP_{z3}= 0.328	$z3_{\Omega_N}$=[21.03]	
6	u_{z4} = 81.12 : ΔP_{z4} = 60	u_{z5} = 72.02	$z4_{\Omega_N}$= [0]	986.67
	u_{z5} = 72.02 : ΔP_{z5} = 42.24	ΔP_{z5}= 13.408	$z5_{\Omega_N}$= [965.64]	
	u_{z6} = -.- : ΔP_{z6} = 0.0		$z6_{\Omega_N}$= [0]	
	u_{z1} = 75.51 : ΔP_{z1} = 0.8		$z1_{\Omega_N}$= [0,0]	
	u_{z2} = 58.90 : ΔP_{z2} = 0.35		$z2_{\Omega_N}$= [19.67]	
	u_{z3} = 73.36 : ΔP_{z3} = 66.63	u_{z2} = 58.90	$z3_{\Omega_N}$= [0]	
		ΔP_{z2} = 0.334		
7	u_{z4} = 64.19 : ΔP_{z4} = 1.693	u_{z6} = 72.02	$z4_{\Omega_N}$= [0]	982.79
	u_{z5} = 81.12 : ΔP_{z5} = 60	ΔP_{z6} = 13.373	$z5_{\Omega_N}$= [0]	
	u_{z6}= 72.02 : ΔP_{z6} = 42.24		$z6_{\Omega_N}$= [963.12]	
	u_{z7} = -.- : ΔP_{z7} = 0.0		$z7_{\Omega_N}$= [0]	
	u_{z1} = 75.51 : ΔP_{z1} = 0.8		$z1_{\Omega_N}$= [0,0]	
	u_{z2} = 58.90 : ΔP_{z2} = 0.35		$z2_{\Omega_N}$= [19.67]	
	u_{z3} = 73.36 : ΔP_{z3} = 66.63	u_{z2} = 58.90	$z3_{\Omega_N}$= [0]	
		ΔP_{z2} = 0.334		
8	u_{z4} = 56.87 : ΔP_{z4} = 0.748	u_{z7} = 72.02	$z4_{\Omega_N}$= [0,0]	982.79
	u_{z5} = 64.19 : ΔP_{z5} = 0.945	ΔP_{z7} = 13.373	$z5_{\Omega_N}$= [0,0]	
	u_{z6} = 81.12 : ΔP_{z6} = 60		$z6_{\Omega_N}$= [0]	
	u_{z7} = 72.2 : ΔP_{z7} = 42.24		$z7_{\Omega_N}$= [963.12]	

	u_{z8} = -.- : ΔP_{z8} = 0.0		$z8_{\Omega_N}$= [0]	
	u_{z1} = 64.19 : ΔP_{z1} = 0.945 u_{z2} = 56.87 : ΔP_{z2} = 0.748 u_{z3} = 81.12 : ΔP_{z3} = 60 u_{z4} = 57.04 : ΔP_{z4} = 0.287 u_{z5} = 75.51 : ΔP_{z5} = 0.513 u_{z6} = 58.90 : ΔP_{z6} = 0.35 u_{z7} = 73.36 : ΔP_{z7} = 66.63 u_{z8} = 72.02 : ΔP_{z8} = 42.24 u_{z9} = -.- : ΔP_{z9} = 0.0	u_{z6} = 58.90 ΔP_{z6} = 0.334 u_{z8} = 72.02 ΔP_{z8} = 13.373	$z1_{\Omega_N}$= [0] $z2_{\Omega_N}$= [0] $z3_{\Omega_N}$= [0] $z4_{\Omega_N}$= [0] $z5_{\Omega_N}$= [0] $z6_{\Omega_N}$= [19.67] $z7_{\Omega_N}$= [0] $z8_{\Omega_N}$= [963.12] $z9_{\Omega_N}$= [0]	
9 (10)				982.79
11	u_{z1}= 72.02 : ΔP_{z1} = 42.24 u_{z2}= -.- : ΔP_{z2} = 0.0 u_{z3}= 58.9 : ΔP_{z3} = 0.35 u_{z4}= 57.04 : ΔP_{z4} = 0.287 u_{z5}= 75.51 : ΔP_{z5} = 0.513 u_{z6}= 73.36 : ΔP_{z6} = 66.63 u_{z7}= 81.12 : ΔP_{z7} = 60 u_{z8}= 52.13 : ΔP_{z8} = 0.393 u_{z9}= 64.19 : ΔP_{z9} = 0.552 u_{z10}= 50.07 : ΔP_{z10} = 0.334 u_{z11}= 56.87 : ΔP_{z11} = 0.414	ΔP_{z1} = 7.49 ΔP_{z3} = 0.35 ΔP_{z4} = 0.287 ΔP_{z6} = 3.152 ΔP_{z8} = 0.393 ΔP_{z9} = 0.552 ΔP_{z10} = 0.334 ΔP_{z11} = 0.414	$z1_{\Omega_N}$= [539.43] $z2_{\Omega_N}$= [0] $z3_{\Omega_N}$= [20.62] $z4_{\Omega_N}$= [16.37] $z5_{\Omega_N}$= [0] $z6_{\Omega_N}$= [231.23] $z7_{\Omega_N}$= [0] $z8_{\Omega_N}$= [20.49] $z9_{\Omega_N}$= [35.43] $z10_{\Omega_N}$= [16.72] $z11_{\Omega_N}$= [23.54]	903.83